The Meteoritical Society

Meteoritics & Planetary Science 45, Nr 10–11, 1590–1617 (2010)
doi: 10.1111/j.1945-5100.2010.01153.x

Almahata Sitta (= asteroid 2008 TC_3) and the search for the ureilite parent body

Peter JENNISKENS[1*], Jérémie VAUBAILLON[2], Richard P. BINZEL[3], Francesca E. DEMEO[3,4], David NESVORNÝ[5], William F. BOTTKE[5], Alan FITZSIMMONS[6], Takahiro HIROI[7], Franck MARCHIS[1], Janice L. BISHOP[1], Pierre VERNAZZA[8], Michael E. ZOLENSKY[9], Jason S. HERRIN[9], Kees C. WELTEN[10], Matthias M. M. MEIER[11], and Muawia H. SHADDAD[12]

[1]Carl Sagan Center, SETI Institute, 189 Bernardo Ave., Mountain View, California 94043, USA
[2]Observatoire de Paris, I.M.C.C.E., 77 Av. Denfert Rochereau, Bat. A., FR-75014 Paris, France
[3]Department of Earth, Atmospheric, and Planetary Sciences, Massachusetts Institute of Technology, 77 Massachusetts Ave., Cambridge, Massachusetts 02139–4307, USA
[4]Observatoire de Paris, L.E.S.I.A., 5 Place Jules Janssen, FR-92195 Meudon, France
[5]Department of Space Studies, Southwest Research Institute, 1050 Walnut St., Suite 400, Boulder, Colorado 80302, USA
[6]Astrophysics Research Centre, School of Mathematics and Physics, Queen's University Belfast, Belfast BT7 1NN, UK
[7]Department of Geological Sciences, Brown University, Providence, Rhode Island 02912, USA
[8]ESA, ESTEC, Keplerlaan 1, NL-2200 AG Noordwijk, The Netherlands
[9]NASA Johnson Space Center, 2101 NASA Parkway, Houston, Texas 77058, USA
[10]Space Sciences Laboratory, University of California, Berkeley, California 94720–7450, USA
[11]Department of Earth Sciences, E.T.H. Zurich, CH-8092 Zurich, Switzerland
[12]Department of Physics and Astronomy, University of Khartoum, P.O. Box 321, Khartoum 11115, Sudan
[*]Corresponding author. E-mail: pjenniskens@mail.arc.nasa.gov

(Received 28 November 2009; revision accepted 25 October 2010)

Abstract–This article explores what the recovery of 2008 TC_3 in the form of the Almahata Sitta meteorites may tell us about the source region of ureilites in the main asteroid belt. An investigation is made into what is known about asteroids with roughly the same spectroscopic signature as 2008 TC_3. A population of low-inclination near-Earth asteroids is identified with spectra similar to 2008 TC_3. Five asteroid families in the Main Belt, as well as a population of ungrouped asteroids scattered in the inner and central belts, are identified as possible source regions for this near-Earth population and 2008 TC_3. Three of the families are ruled out on dynamical and spectroscopic grounds. New near-infrared spectra of 142 Polana and 1726 Hoffmeister, lead objects in the two other families, also show a poor match to Almahata Sitta. Thus, there are no Main Belt spectral analogs to Almahata Sitta currently known. Space weathering effects on ureilitic materials have not been investigated, so that it is unclear how the spectrum of the Main Belt progenitor may look different from the spectra of 2008 TC_3 and the Almahata Sitta meteorites. Dynamical arguments are discussed, as well as ureilite petrogenesis and parent body evolution models, but these considerations do not conclusively point to a source region either, other than that 2008 TC_3 probably originated in the inner asteroid belt.

INTRODUCTION

On October 7, 2008, a small 3–4 m-sized asteroid called 2008 TC_3 impacted Earth's atmosphere over the Nubian Desert of northern Sudan (Kowalski 2008). The asteroid was classified as belonging to taxonomic class F, meaning "flat" (Tholen 1984), based on the flat shape of the 550–1000 nm reflectance spectrum, measured prior to impact, and the 300–2500 nm reflectance spectra of the earliest recovered meteorites (Jenniskens et al. 2009).

Meteorites collectively called Almahata Sitta were recovered in the following months, scattered along the approach path of the asteroid. Most of these fragments

© The Meteoritical Society, 2010.

were ureilites of a wide range of types, some anomalously porous compared to known ureilites. Thus, Almahata Sitta was classified as an anomalous polymict ureilite (Zolensky et al. 2010). This provided the first firm link between a meteorite type and an asteroid taxonomic class (Jenniskens et al. 2009).

The result was surprising, because ureilites were traditionally linked to S-class (S for "stony") asteroids of subtype III (Gaffey et al. 1993; Sandford 1993; Burbine et al. 2002), mainly based on ordinary chondrite like visible slopes in ureilite reflectance spectra now understood to be the result of terrestrial weathering. For a comparison of Almahata Sitta reflectance spectra with S-class asteroid spectra, see Hiroi et al. (2010). Before this link was made, F- and B-class asteroids (B for "blue-sloped") did not seem to have meteorite analogs (Britt et al. 1992), or were linked to partially altered carbonaceous meteorites that are now thought to have better spectral analogs among K-complex asteroids, instead (Clark et al. 2009).

In this article, we explore this link further and attempt to use the first recovery of samples from a known asteroid to search for the source region of ureilites in the asteroid belt. At first, this may seem an easy task, because the rarity of F-class asteroids (only 4%, 92 of ~2000 classified asteroids) and ureilites (only ~0.6% of meteorite falls, 6 of 987) suggests that the source region in the asteroid belt is a spectral anomaly. Also, ureilites appear to have an unusual petrogenesis and protoplanet evolution that may provide additional insight into the source region.

The obvious approach would be to compare the spectrum of 2008 TC_3 to that of other asteroids and select those that are most similar. In practice, however, meteorite reflectance spectra are not necessarily the same as asteroid reflectance spectra, and near-Earth asteroids (NEA) surfaces can differ from those of their parent asteroids in the Main Belt. For example, Q-class asteroids are found in the Main Belt only in very young < 1 Myr families (Mothé-Diniz and Nesvorný 2008), but are common among NEA (e.g., McFadden et al. 1984; Fevig and Fink 2007), where they appear to be examples of S-class asteroids that have had their regolith disturbed and possibly overturned by gravitational perturbations from close encounters with Earth (Binzel et al. 2010a). In addition, many aspects of ureilite petrogenesis and protoplanet evolution are too controversial and model-dependent to provide firm constraints.

Linking Meteorite Types to Asteroid Taxonomic Classes

Earlier attempts to identify parent bodies of particular meteorite groups in the Main Belt have been hampered by the fact that the larger Main Belt asteroids can be covered in different degrees by a layer of light-scattering dust and regolith, scattering blue light more than red, and thus causing a blue-tilted slope in reflectance spectra (Gaffey et al. 1993; Burbine et al. 2002). 2008 TC_3, however, had a reflection spectrum very similar to that of the freshly fallen meteorites (Jenniskens et al. 2009; Hiroi et al. 2010), possibly because this small tumbling asteroid rotated too fast to hold on to surface regolith (Scheirich et al. 2010).

In addition, asteroid surfaces are irradiated by cosmic rays and solar wind, a process called space weathering, and are bombarded by micrometeorites, a process called impact gardening. Space weathering causes nanophase iron to separate out of minerals, changing the surface reflectivity over time (lowering the asteroid's geometric albedo for high albedo asteroids, or raising the albedo for dark asteroids), and typically red-tilting the reflectance slope at optical wavelengths and somewhat less so at near-infrared (IR) wavelengths (Hiroi et al. 1999; Sasaki et al. 2002; Strazzulla et al. 2004; Brunetto et al. 2006; Marchi et al. 2006; Willman et al. 2010). This process was first documented for the Moon (e.g., Pieters et al. 1993, 2000; Noble and Pieters 2003) and then observed for Mercury (Hapke 2001) and asteroids (e.g., Clark et al. 2002; Brunetto et al. 2006). Because the 2008 TC_3 asteroid spectrum was so similar to that of the recovered meteorites, space weathering must not have affected the surface much in this wavelength range. 2008 TC_3 broke off from a larger asteroid only 19.5 ± 2.5 Ma, based on cosmic ray exposure (CRE) time (Welten et al. 2010). By contrast, the Main Belt progenitor of 2008 TC_3 was exposed for a much more significant period of time before the impact occurred that broke off 2008 TC_3. Sadly, nothing is known about how space weathering changes the reflectance properties of ureilites.

The reflectance spectra of asteroids can also be changed by thermal metamorphism (e.g., Clark et al. 1992; Hiroi et al. 1993; Ohtsuka et al. 2009), although this is unlikely to be a concern in this case because 2008 TC_3 did not come close to the Sun in its recent orbital evolution (see below). A more realistic, common concern is terrestrial weathering of the meteorites. Terrestrial weathering rusts metallic iron into limonite (iron oxides and hydroxides) with strong near-UV and 900 nm absorption bands (Cloutis et al. 2010; Hiroi et al. 2010). However, Almahata Sitta is the first polymict ureilite not severely affected by terrestrial weathering (Zolensky et al. 2010).

Other aspects that complicate linking meteorites to their parent bodies in the Main Belt include inhomogeneity in the asteroid progenitors on a macroscopic scale. Indeed, the recovered Almahata Sitta

meteorites showed much diversity in texture and albedo (Jenniskens et al. 2009). In addition, some 20–30% in mass of recovered Almahata Sitta meteorites are found to consist of anomalous (nonureilite) meteorites, which included H5 and L4 ordinary chondrites, and EH6 and EL6 enstatite chondrites (Shaddad et al. 2010; Zolensky et al. 2010). These did not originate from prior falls in the area, but were part of 2008 TC_3, based on their low terrestrial weathering levels (Zolensky et al. 2010), similar mass distribution in the strewn field to that of the ureilites (Shaddad et al. 2010), and because sample #25 (H5) carried a similar polyaromatic hydrocarbon molecular fingerprint as the Almahata Sitta ureilites, presumably from cross-contamination in the asteroid (Sabbah et al. 2010). Also, the cosmogenic radionuclides in samples #25 (H5 chondrite) and #A100 (L4 chondrite) indicated that both chondrites came from a (rare among falls) large object with a radius of approximately 300 g cm^{-2} (which corresponds to diameter $D \sim 3.5$ m if the density = 1.7 g cm^{-3}), which is identical to the preatmospheric size derived from the Almahata Sitta ureilites (300 ± 30 g cm^{-2}). Sample #25 came from a depth of 100–150 g cm^{-2}, whereas sample #A100 came from closer to the surface (<50 g cm^{-2}). Both chondrites show a CRE age of 23 ± 2 Myr, based on the $^{21}Ne/^{26}Al$ method, which overlaps within measurement error with the average CRE age of 19.5 ± 2.5 Myr for the Almahata Sitta ureilites (Welten et al. 2010). Fortunately, the flat visible slope of the observed astronomical spectrum of 2008 TC_3 implies that these anomalous meteorite types did not dominate the reflectance properties of the asteroid in the observed wavelength range.

Ureilite Petrogenesis and Protoplanet Evolution

The source region of ureilites in the Main Belt is of particular interest. At present, few meteorite source regions are known: the L chondrites are thought to be associated with the Gefion family (Nesvorný et al. 2009), the howardite, eucrite, and diogenite (HED) clan of meteorites has been identified, still somewhat tentatively, as originating from the Vesta asteroid family, a group of differentiated asteroids (e.g., Burbine et al. 2001; Duffard et al. 2004; Moskovitz et al. 2008, 2010), and the LL chondrites appear to be a good match with the Flora family in the inner Main Belt (Vernazza et al. 2009).

Ureilites, albeit rare, are the second most common type of achondrites after HED meteorites. They are generally considered to be primitive achondrites, with a petrogenesis that in some way bridges the evolutionary gap between primitive chondrites and fully differentiated asteroidal bodies. In addition, they are thought by many researchers to have derived from a single parent body, here referred to as the ureilite parent body (UPB). This is suggested by the fact that olivine and pyroxene clasts in polymict ureilites have the same range of chemical and oxygen isotopic compositions as found in unbrecciated ureilites (Downes et al. 2008), and that all ureilites share a common thermal history (Goodrich 2004). These properties appear to hold for the population of ureilite samples in Almahata Sitta as well (Herrin et al. 2010; Rumble et al. 2010; Zolensky et al. 2010). Of course, only a small fraction of all 259 known ureilites (falls and finds) have been studied in sufficient detail to be certain that they come from a single body. Those that have, create a picture of a UPB that was heterogeneous in mg# (molar Mg/Mg + Fe), pyroxene abundance and type, and oxygen isotopic composition, with a rapid extraction of melt that preserved much of this heterogeneity and prevented wholesale metal/silicate fractionation (Goodrich 2004; Goodrich et al. 2007; Warren and Kallemeyn 1992; Warren and Huber 2006).

For review articles on the topic of ureilites, see Vdovykin (1970), Berkley et al. (1980), Dodd (1981), Takeda (1987), Takeda et al. (1989), Goodrich (1992), Mittlefehldt et al. (1998), Singletary and Grove (2003), Goodrich (2004), Mittlefehldt (2005), Warren and Huber (2006), and Wilson et al. (2008). The mineralogy and petrology of Almahata Sitta are described by Zolensky et al. (2010) and Herrin et al. (2010), whereas other aspects of elemental and isotopic compositions are given in the articles by Friedrich et al. (2010), Rumble et al. (2010), and Qin et al. (2010). In brief, ureilites consist predominantly of magnesian olivine, low- and high-Ca pyroxene, including pigeonite, graphite, diamond, high-Cr troilite, silica, and metal. A characteristic feature of ureilites is that olivine grains exhibit high mg# rims, the result of a high-temperature in situ reduction event of short duration, commonly interpreted to have been caused by catastrophic disruption of the parent body in a giant collision (Berkley et al. 1980; Warren and Kallemeyn 1992; Singletary and Grove 2003). This collision also resulted in conversion of graphite to diamonds at high shock pressure (Vdovykin 1970). Fragments reassembled and underwent subsequent collisions. Almahata Sitta contains both the porous aggregates of ureilite-like grains as found in polymict ureilites, and course-grained igneous material characteristic of main group (unbrecciated) ureilites. Although some aspects of Almahata Sitta samples are anomalous, there is no indication that they do not originate from the same original parent body as main group ureilites, an aspect that is discussed in more depth in Herrin et al. (2010).

A plausible history of ureilite petrology and parent body evolution is summarized in the cartoon shown in

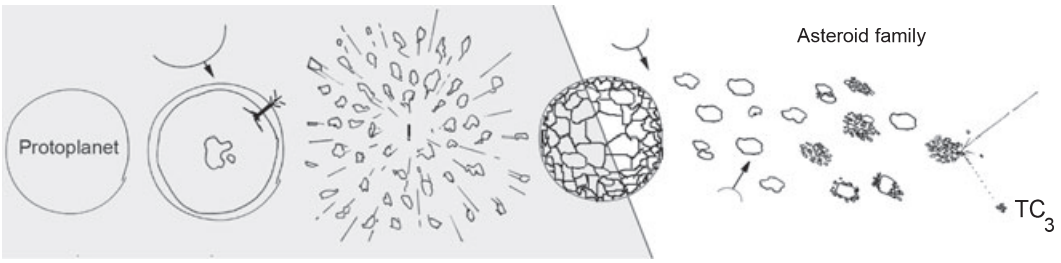

Fig. 1. Cartoon summarizing our understanding of the origin and evolution of the ureilite parent body. From left to right: The ureilite parent body protoplanet underwent partial melting and melt-extraction before a catastrophic disruption occurred that created 10–100 m-sized fragments. The fragments reassembled and migrated to the current position in the asteroid belt; In more recent times, a collision broke the protoplanet and created an asteroid family. The daughter asteroids broke and fragments underwent size reduction to centimeter-size scale in multiple collisions, each time followed by a process of reaccretion into asteroids, during which chondritic material became mixed in with the ureilitic material. More recently, a small asteroid collided with the parent asteroid of 2008 TC_3 and released the 3 m object, now exposed to cosmic rays. The small asteroid evolved into a mean-motion resonance and was perturbed into an Earth-crossing orbit, from which it impacted Earth and was recovered.

Fig. 1 (after Downes et al. 2007; Herrin et al. 2010). The textures, mineralogy, and depleted trace element composition of ureilites suggest an origin in a partially melted (basalt-depleted) asteroidal mantle of a carbon-rich protoplanet, the size of which is debated (Wilson et al. 2008). At the end of the igneous period, when some melt was still present, the UPB experienced a giant collision that shattered the mantle into 10–100 m-sized pieces (Herrin et al. 2010) and extracted the rest of the melt rapidly. The role of smelting (C-controlled reduction of FeO out of silicates) in the evolution of the UPB is highly controversial. It may have been responsible for the "primary" heterogeneity of UPB materials (Singletary and Grove 2003; Goodrich et al. 2007), or it may only have operated as a runaway process in the late stages of planetary breakup (Warren and Huber 2006).

Most workers agree that after the giant collision, the fragments of the UPB reassembled into a jumbled state, possibly around the remnant of the original body. That body was subsequently hit to produce a family of daughter asteroids, a process that was repeated more than once over the history of the solar system, given the collisional evolution needed to get from approximately 10 m-sized UPB fragments to some of the finer grained clasts found in Almahata Sitta.

Based on the presence of nonureilitic material in Almahata Sitta, material originating from different parent bodies must have become mixed in. Some 10–15% of ureilites are polymict (breccias), which often contain exotic (nonureilite) lithic and mineral clasts (Gaffey et al. 1990; Goodrich 2004; Downes et al. 2008; Rankenburg et al. 2008). Almahata Sitta, especially, contained 20–30% (in mass) of foreign materials, most at the centimeter-size scale (Shaddad et al. 2010). Given that centimeter-sized fragments are quickly removed from the general asteroid population by nongravitational forces (i.e., a combination of Poynting-Robertson drag and the Yarkovsky effect), some of these fragments may have originated in the impactors, providing insight into the collisional environment over time.

We know that the Almahata Sitta meteorites came from asteroid 2008 TC_3. In the NEA Similar to 2008 TC_3 section we identify a number of other NEA with spectra similar to 2008 TC_3 and investigate the dynamical pathway from asteroid belt to the near-Earth environment. Two groups are identified with similar spectra, moving in low- and high-inclination orbits, which appear to originate from two different sources. 2008 TC_3 had a low-inclination group like that of the former. In the Main Belt Asteroids Similar to 2008 TC_3 section, we identify five potential source regions in the Main Belt, as well as a population of ungrouped asteroids with similar spectra scattered throughout the inner and central belt. Their potential as a source for ureilites is investigated. Finally, we evaluate Main Belt asteroid groups and their potential as the most likely source regions of 2008 TC_3 considered in the Discussion section.

NEA SIMILAR TO 2008 TC_3

The Reflectance Spectrum of 2008 TC_3

The observed asteroid reflectance spectrum (Fig. 2, top) was spectrally flat (gray) at 550–800 nm wavelengths and had a weak pyroxene absorption band around 900 nm. No near-IR spectrum was measured. The absolute scale of the spectrum, the geometric albedo of the asteroid, was not measured. For that reason, the result is plotted as a "relative reflectance" on a logarithmic scale in Fig. 2 (and subsequent figures), so that each spectrum will shift up and down along the *Y*-axis by multiplying with a scale factor without affecting the shape of the spectrum if the particular scale value (e.g., albedo) is changed.

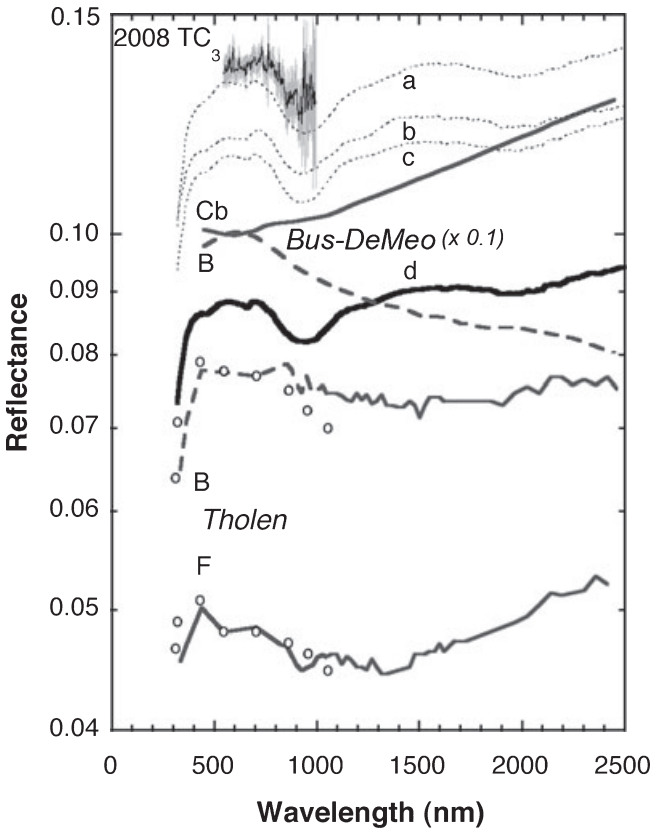

Fig. 2. The measured astronomical reflectance spectrum of 2008 TC_3 (top, Jenniskens et al. 2009). Below that, composite average spectra derived from Almahata Sitta meteorites are shown as dotted curves (labeled a–c), and the thick solid curve labeled "d" (Hiroi et al. 2010). Results are compared to the average spectra of the four Bus-DeMeo (top) and Tholen (bottom) taxonomy classes with a flat slope in the visual regime. The Bus-DeMeo taxonomy mean spectra for Cb and B classes are normalized to 0.1 at 500 nm (DeMeo et al. 2009). The Tholen taxonomy mean spectra for F and B classes are from Tholen and Barucci (1989), open dots, which were scaled to absolute reflectances by Hiroi et al. (2001), solid line.

Outside the 550–1000 nm range, the recovered meteorites provide insight into the asteroid's spectral reflectance. The recovered meteorites exhibit a range of reflectance spectra due to large variations of olivine/pyroxene ratios and carbon content on a millimeter–centimeter-sized scale, the spot size of the measurements. This spectral diversity from one meteorite to the next is discussed in Hiroi et al. (2010). All meteorites show a flat visual and near-IR spectrum and most have a weak pyroxene band near 900 nm. Some show olivine bands at approximately 1100 nm and below 500 nm. Other possible combinations show a stronger olivine band signature and slightly different slope in the near-UV and near-IR. Individual meteorite spectra show a range of weak pyroxene (at 900–1000 nm) and olivine (at 1000–1600 nm) bands, often with a weak downturn short of 500 nm and a stronger downturn below 400 nm (Hiroi et al. 2010, and discussion therein).

The astronomical spectrum provides a strong constraint on which combination of Almahata Sitta meteorites is a reasonable analog to the asteroid spectrum over a wider wavelength range. Dotted lines in Fig. 2 (labeled a–c) show the range of possible blue and near-IR spectral shapes based on combinations of reflectance spectra from five individual Almahata Sitta meteorites (#4, 7, 25, 27, and 47; Hiroi et al. 2010), all measured at 19° incidence and 0° emergence angles (as was asteroid 2008 TC_3). All are classified as ureilites, except sample #25, which is an H5 chondrite. Combinations were chosen in such a manner that the sum provides a fit to the observed spectrum. Spectrum "c" is the least-squares fit match discussed by Hiroi et al. (2010) and is composed of 75% #4, 16% #25, and 8% #27. In comparison, spectrum "a" is composed of 15% #4, 27% #7, 4% #25, 3% #27, and 52% #47, whereas spectrum "b" is composed of 29% #4, 14% #7, 0%#25, 29% #27, and 29% #47. The albedo values measured by Hiroi et al. (2010) were a factor of 2 higher than those measured by Jenniskens et al. (2009). The reason for this discrepancy was not resolved.

Spectrum "d" is the same as spectrum "b," scaled arbitrarily to the albedo measured for sample #7 by Jenniskens et al. (2009). The actual albedo is likely within a factor of 2 of this value. We will reproduce this spectrum in upcoming figures as a reference.

Other parts of the spectra are important as well. No 10 μm (Si-O) bands typical of hydrated silicates were detected at mid-IR wavelengths and only a weak 3 μm (O–H) band from adsorbed telluric water in some cases (Hiroi et al. 2010; Sandford et al. 2010). No hydrated minerals were identified in petrology and mineralogy studies (Zolensky et al. 2010). Hence, Almahata Sitta meteorites are dry ($<<1\%$ hydrated silicates), and so presumably was asteroid 2008 TC_3.

Retrieving Reflectance Spectra from Asteroids Taxonomic Databases

Relatively, few asteroids have known reflectance spectra over the full 350–2500 nm range. Most spectroscopic information is derived from broadband photometric surveys, providing spectral information at a low spectral resolution over a less-than-ideal wavelength range. The comparison of those data to the spectrum of 2008 TC_3 (and Almahata Sitta composites) is made easier by the fact that the sorting of asteroid spectra into groups that describe the full range of spectral diversity has already been done. This has resulted in several taxonomy schemes, the specific classification criteria depending on the data set used.

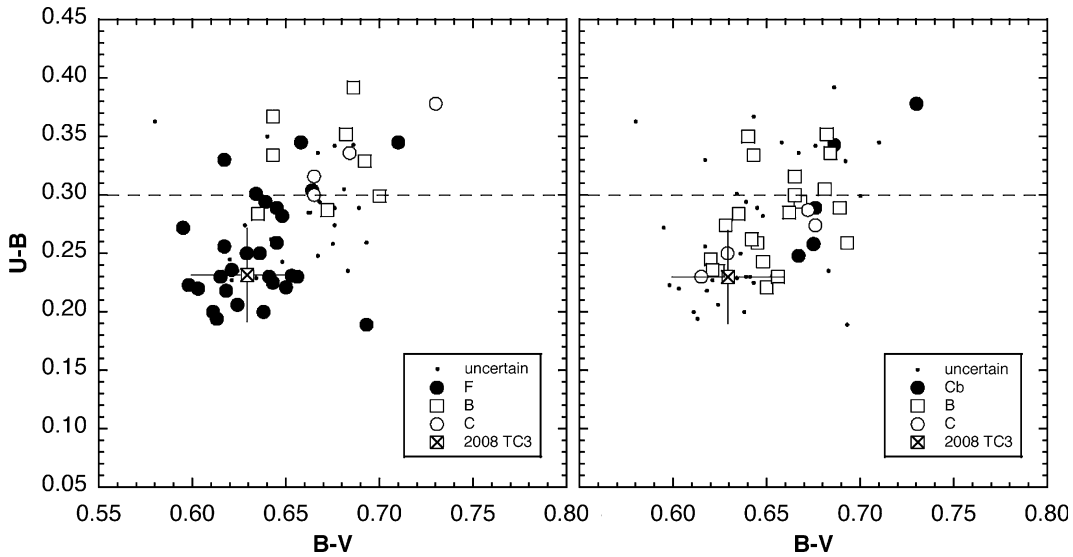

Fig. 3. Colors of 2008 TC_3 in a two-color diagram. Left: asteroids classified as F and B class in the Tholen taxonomy, including four C-class asteroids that were classified as B class in the SMASII survey. Right: asteroids classified as B and Cb class in the Bus–DeMeo taxonomic scheme. Small dots (uncertain) are all others with unknown or intermediate classifications in either taxonomic scheme. In calculating the photometric colors from the reflectance values of Fig. 2, it was taken into account that the Sun (a G2V star) has (B–V) = 0.65 ± 0.02 and (U–B) = 0.17 ± 0.03 (Croft et al. 1972; Tedesco et al. 1982b; Gray 1992; Straizys and Valiauga 1994).

The two most commonly applied taxonomy schemes are that of Tholen (1984) and Tholen and Barucci (1989), based on eight-channel photometric data (Zellner et al. 1985), and that of Bus (Bus 1999; Bus and Binzel 2002) and DeMeo (DeMeo et al. 2009), based on visible and near-IR spectra of asteroids obtained by CCDs in the Small Mainbelt Asteroid Spectroscopic Survey (SMASS) and SMASSII surveys, after extending the spectral data into the near-IR, beyond the range defined by the Tholen taxonomy. The identification of spectra similar to 2008 TC_3 then boils down to selecting asteroids of the same taxonomic class as 2008 TC_3.

The problem with this approach is that the two different taxonomic schemes do not isolate the same clusters of spectral shapes. In Fig. 2, the Almahata Sitta spectrum is compared to mean spectra for the two classes that most resemble 2008 TC_3 in the Tholen (F and B) and Bus-DeMeo taxonomy (Cb and B). These spectra are derived predominantly from Main Belt objects.

In the Tholen taxonomy, B- and F classes were assigned originally to extensions in the common C-class group in the cluster analysis of asteroid spectroscopic data (Tholen 1984). The F-class spectrum is relatively flat at visible wavelengths, whereas B-class spectra have a more bluish slope. In practice, there is much confusion between F and B class asteroids (Cellino et al. 2002; Clark et al. 2010). Indeed, while the average slope by Tholen and Barucci (1989), shown as open symbols in Fig. 2, is more flat for the F-class asteroids (hence the classification of 2008 TC_3 as an F-class asteroid), the same is no longer true for the average asteroid spectra assembled by Hiroi et al. (2001), shown as a solid line in Fig. 2. Now, F- and B-class asteroids have the same slope and similar near-UV absorption. The difference is mainly caused by observers who take albedo into account in discriminating between F- and B-class asteroids. Although the F-class asteroids tend to have lower albedo than most B-class asteroids, this is not always the case. In detail, F-class asteroids show a wide variety of spectral shapes in the near-IR (see below). Also, some F-class asteroids show 3 μm OH-stretching vibrational bands distinctive of hydrated silicates, whereas others do not (Jones et al. 1990; Gaffey et al. 1993), suggesting that F-class asteroids can represent more than one type of meteorite.

The difference between Tholen B- and F-class asteroids is apparent in the (B–V) and (U–B) photometric colors of the asteroids (Fig. 3). The mean wavelengths of the Johnson photometric pass bands U, B, and V (Johnson and Morgan 1953) are at 364, 442, and 540 nm (central wavelength at 356, 444, and 548 nm, respectively), respectively. The spectral slope (= the colors) are expressed as differences in stellar magnitude measured for each pass band, e.g., (B–V) or (U–B). Those with (U–B) > 0.30 tend to be classified as B in the Tholen taxonomy, having a steeper blue-tilted slope at ultra-violet to visible wavelengths.

In the Bus taxonomy scheme (Bus 1999; Bus and Binzel 2002), the only flat visible spectra (usually

provided by normalization to 1.0 at 500 nm) are those of Cb- and B-class asteroids (Fig. 2), where B class in the Tholen classification does not necessarily represent the same objects as B class in the Bus classification. Both classes have a wide range of albedos. The reason why the Tholen F class does not survive as a unique grouping in the Bus taxonomy is because of a lack of 350–450 nm range ultraviolet spectroscopic information in the SMASSII spectral survey. This system was later refined by DeMeo et al. (2009) to the Bus-DeMeo taxonomy, based on the near-IR (900–2500 nm) reflection spectra, now showing distinct slopes at near-IR wavelength, with the Almahata Sitta meteorites suggesting an intermediate case (Fig. 2). This makes the Cb and B taxonomy a useful way to search for 2008 TC_3 like asteroidal spectra, but the spectra thus selected cannot be interpreted as necessarily the same.

Figure 3 shows the general compatibility of the Bus-DeMeo B class and the Tholen F class in the domain of (U–B) versus (B–V). When no U-band (365 nm) photometry is available, a negative or flat near-IR slope and a weak downturn of relative reflectance below 500 nm are indicative of being consistent with the Tholen definition of F class. Hence, the color (B–V) < 0.66 can be used to identify more Tholen F-class asteroids among the Bus B and Cb classes. The F-class spectra are those with a flat or blue slope at 500–800 nm wavelengths (no redder than 1% over this wavelength range) and a relative reflectance (normalized at 1.0 at 500 nm) between B and V of < 1.01.

The blue (meteorite-based) part of the composite spectrum of 2008 TC_3 plots among the F-class asteroids at (B–V) = +0.63 ± 0.03 and (U–B) = +0.23 ± 0.04 magnitudes (Fig. 3). For reference purposes in future work, other photometric colors derived from the composite Almahata Sitta meteorite spectrum are: (V–R) = +0.35, (V–I) = +0.66, (V–J) = +1.16, (J–H) = +0.35, and (H–K) = +0.06. Here, we used the standard photometric pass band systems of Johnson (U, B, V), Cousins (R, I), and Mauna Kea (J, H, K).

NEA Similar to 2008 TC_3

Other ureilitic objects released from the same source region in the past few tens of Myr should be found along an evolutionary path close to the perihelion distance q = 1.0 AU line, having low inclination and a reflectance spectrum not unlike 2008 TC_3 itself, for the following reasons. Just before impact, 2008 TC_3 moved in a low-inclination orbit (i = 2.54220 ± 0.00004°) that stretched from a perihelion just inside Earth's orbit (q = 0.899957 ± 0.000002 AU) to an aphelion (Q = 1.72 AU) just outside the orbit of Mars, with semimajor axis a = 1.308201 ± 0.000009 AU (Jenniskens et al. 2009). By tracking the asteroid for 20 h, the orbit of 2008 TC_3 was calculated 10,000 times better than the typical orbits derived from fireball observations alone (Jenniskens et al. 1992). That still limits the accuracy at which the orbit can be integrated backward in time. The Lyapunov time scale is of order approximately 1000 yr, signifying the exponential rate at which nearby trajectories diverge, but the dynamical lifetime of the orbit of 2008 TC_3-like asteroids (since ejection from the asteroid belt) is a few Myr to many tens of Myr or longer (Gladman et al. 1996; Bottke et al. 2002a, 2002b). Indeed, 2008 TC_3 broke from a parent object about 19.5 Ma, as mentioned earlier (Welten et al. 2010). This is in the 1.1–32.3 Myr range of other ureilites (Aylmer et al. 1990).

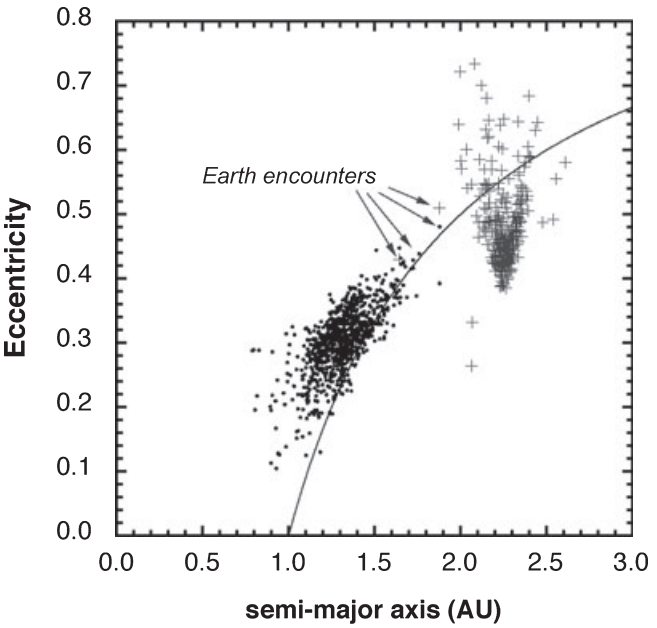

Fig. 4. Diagram of orbital elements for clones of 2008 TC_3 (•) and 1998 KU_2 (+). The asteroid orbits were integrated back 102,497 yr, and then clones were integrated forward to the present time. The solutions most affected by Earth encounters are marked.

To create a statistical picture of possible orbital pathways and search for a trail of crumbs that shows this orbital evolution, we integrated the orbit of 2008 TC_3 back over a period of approximately 102,500 yr (~100 Lyapuov time scales), created 1000 orbit clones distributed within the uncertainty ellipse of the orbital elements, and integrated those orbit clones forward to the present time. The adopted uncertainties (above) were slightly larger than the actual uncertainties because they were assumed to be independent. Figure 4 shows that 2008 TC_3 was in a relatively stable orbit over the short time span of the integrations. There was only a gradual spreading of the solutions along the q = 1.0 AU line,

suggesting that close encounters with Earth were the dominant cause of secular orbital evolution in this time interval. The inclination remained low, because Earth is not efficient at increasing the asteroid's inclination, and because mean-motion resonances did not play a big role in the orbital evolution over this time scale.

Once a collision released 2008 TC_3 from its parent body (Fig. 1, right side), it most likely needed the Yarkovsky effect to evolve its semimajor axis into a mean-motion resonance (Bottke et al. 2002a). Once in the resonance, the asteroid followed chaotic orbits and was quickly ejected into a more eccentric orbit, until crossing Earth's orbit where the orbit was decoupled from the resonance (Wisdom 1987). Hence, it is expected that the orbit of 2008 TC_3 was more elliptical in the past. Only two solutions of 1000 possible past orbits of 2008 TC_3 show a significantly higher eccentricity 100,000 yr in the past. This would make such evolution an unlikely event over a period of 100,000 yr, needing a time scale of tens of Myr instead. Given that 2008 TC_3 broke off a larger asteroid only 19.5 Ma, this suggests that 2008 TC_3 spend much of the time since breakup outside the Main Belt, evolving into its recent, Earth-impacting orbit.

Using a different method, we applied the NEO model described in Bottke et al. (2002b) to predict the source region of 2008 TC_3 based on its semimajor axis, eccentricity, and inclination (a, e, i). This is an inexact process for small bodies, but it can be useful to rule out particular source bodies. Assuming that 2008 TC_3 had an (a, e, i) of (1.308 AU, 0.312, and 2.542°), we estimate it had a strong likelihood of coming from the inner Main Belt region. Specifically, we predict the probability that 2008 TC_3 came from the ν_6 secular resonance and/or the significant quantity of Mars- and three-body resonances in the inner Main Belt to be near 80%. It has been shown that most of our NEOs come from this region (e.g., Bottke et al. 2002b). The odds that it came from the 3:1 mean-motion resonance at 2.5 AU in the Main Belt are 20%. The model shows no signs that 2008 TC_3 could have come from the outer Main Belt.

In prior work, two NEA were identified with Cb-, F-, or B-class spectra that have a perihelion distance ± 0.2 AU from $q = 1.0$ AU: 3671 Dionysus (q = 1.007 AU) and 152629 (1998 KU_2) with $q = 1.0079$ AU (Jenniskens et al. 2009). Both objects have been classified as Cb. A third Cb-class NEA, 3833 Calingasta, is still far from Earth's orbit (Table 1). From the archived asteroid spectroscopic data (Table 1), we now find that 1998 KU_2 does have a similar reflectance spectrum to 2008 TC_3 at visible wavelengths (Fig. 5). This is significant, because 1998 KU_2 with $H = +16.5$ magnitude is much larger than 2008 TC_3, and large enough to hold surface regolith. The near-IR reflectance spectrum is not known. The visible spectrum of Dionysus is similar to that of 1998 KU_2, and not different from 3833 Calingasta in the 430–900 nm wavelength range (Fig. 5). All show a flat visible spectrum and a weak pyroxene band.

The remaining (ungrouped) asteroids in low-inclination orbits with Cb-, F-, or B-class spectra are different. Asteroids 7753 and 25330 have a bluer slope, whereas 2001 XS_1 has a redder slope than 2008 TC_3 (Fig. 5).

A second group of NEA with similar spectra is identified if we include inclinations $>15°$. We find that *nearly half* of NEA with B, F, or Cb spectra have a surprisingly high inclination between 22° and 33° (Table 1). These asteroids have similar spectra at optical wavelengths, steeper tilted toward the blue than the group of spectra resembling 2008 TC_3 (Fig. 6). The sole exception is BCF-class asteroid 1508 Kemi, which has a peak around 680 nm. Clark et al. (2010) identified C-class asteroids 2100 Ra Shalom 1 and 2100 Ra Shalom 2 (i = 15.8°) to have similar spectra to asteroid 1508 (not shown here). Among this high-inclination population is asteroid 3200 Phaethon (Dumas et al. 1998; Licandro et al. 2007), the parent body of the Geminid shower (e.g., Jenniskens 2006).

More NEA Similar to 2008 TC_3

In ongoing work to characterize NEA, we have gathered a number of near-IR spectra of asteroids for which no visual reflectance spectra have been obtained yet, and hence no Tholen or Bus taxonomic classification can be derived. Figure 7 shows the spectra in our sample that most resemble that of the Almahata Sitta composite spectrum. These include asteroids 18106, 52768, 85585, 152895, 185851, and 2001 RY_{47} (Table 1). They all show a relatively narrow 1000 nm band and a weak 2000 nm band, with an overall shallow slope in the near-IR. The variation among these spectra is fully accounted for by the diversity of materials in Almahata Sitta (Fig. 2) (Hiroi et al. 2010).

Based on the near-IR spectra alone, the classification of these spectra is not unique. In the DeMeo et al.'s (2009) taxonomy, most would qualify as an uncertain C,X: or Sq:, not neatly fitting into any of these categories (Table 1). The spectra of 2001 RY_{47} and 52768 are unique, because they have a small and shallow band near 900 nm, much less prominent than for typical spectra with this feature. Other spectra in Fig. 7 are more typical, but with a shallower and/or narrower 900 nm band than typically seen, thus providing a better match to the Almahata Sitta spectrum.

Many of these have absolute magnitudes in the range H = 15–18, suggesting that they can hold surface

Table 1. NEA with similar spectra as 2008 TC_3.

Members	a[a] (AU)	e[a]	i[a] (°)	H (mag.)	D (km)	Albedo	Class Tholen	Class DeMeo	Class This study
Low-inclination objects with F-class spectrum (TC_3 group)									
(2008 TC_3)	1.308	0.312	2.542	31.9	0.004	(0.088)	–	–	F3
152679 (1998 KU_2)	2.253	0.552	4.922	16.5	–	–	–	Cb	F3
3671 Dionysus	2.198	0.542	13.543	16.3	1.5	0.16	–	Cb	F3
3833 Calingasta	2.195	0.389	11.999	15.0	–	–	–	Cb	F3
18106 Blume	2.445	0.512	4.220	17.9	–	–	–	Sq,S:[b]	–
52768 (1998 OR_2)	2.392	0.566	5.866	15.7	–	–	–	C,X:[b]	F3:
85585 Mjolnir	1.297	0.356	4.084	21.4	–	–	–	Sq[b]	–
14402 (1991 DB)	1.715	0.403	11.422	18.4	0.6	0.14	–	C	–
152895 (2000 CQ_{101})	2.289	0.494	2.983	18.1	–	–	–	Sq,S[b]	–
185851 (2000 DP_{107})	1.365	0.377	8.670	18.2	–	–	–	L,K[b]	–
(2001 RY_{47})	0.906	0.393	17.610	19.4	–	–	–	C,X:[b]	F3:
High-inclination objects with Fp-class spectrum (Phaethon group)									
1474 Beira	2.734	0.491	26.679	12.7	–	–	FX	Cb	Fp
1508 Kemi	2.770	0.417	28.737	12.0	–	–	BCF	C	ungr.
3200 Phaethon	1.271	0.890	22.183	14.5	5.1	0.107	F	B	Fp
3581 Alvarez	2.771	0.409	28.809	12.1	–	–	–	Cb	Fp
5690 (1992 EU)	2.801	0.379	29.002	12.5	–	–	–	Cb	Fp
6411 Tamaga	2.761	0.419	28.579	13.0	–	–	–	B	Fp
6500 Kodaira	2.758	0.416	29.305	12.5	–	–	–	B	Fp
155140 (2005 UD)[c]	1.275	0.872	28.730	17.3	1.3	(0.107)	F	B	Fp
(1999 CW_8)	2.238	0.598	33.653	18.5	–	–	–	B	Fp
Ungrouped									
(2001 XS_1)	2.672	0.555	10.924	18.8	–	–	–	Cb	Fl
7753 (1988 XB)	1.468	0.482	3.124	18.6	–	–	–	Cb	Fb
25330 (1999 KV_4)	1.541	0.371	14.327	16.8	3.2	0.052	–	B	Fb

[a]Oscular orbital elements. These data were extracted from JPL's Solar System Dynamics Group small-body database.
[b]No optical reflectance data available, making the classification solution uncertain and not unique. The ":" means that the spectra do not fit neatly into a class.
[c]Jewitt and Hsieh (2006).

regolith. All objects have semimajor axis $a < 2.49$ AU. Asteroid 85585 Mjønir and 185851 are in a similar phase of their orbital evolution as 2008 TC_3: they now have low e and low a, but q still close to 1. The new sample includes only one relatively high-inclination object ($i = 17°$), which also has the shortest perihelion distance ($q = 0.550$) and shortest semimajor axis ($a = 0.906$), presumably having been perturbed most severely over time.

MAIN BELT ASTEROIDS SIMILAR TO 2008 TC_3

Taxonomic data were extracted from the JPL Small-Body Database, searching for Bus-DeMeo Cb- and B-class asteroids (85 matching objects) and for Tholen F- and B-class (and intermediary class) asteroids (67 matching objects). Duplicates were removed, leaving 118 objects. Synthetic proper elements and magnitudes were obtained from the *Astdys* database, calculated by Novakovic, Knezevic, and Milani (Knezevic and Milani 2003) and updated and released on July 2009. This database contains 209,558 numbered asteroids.

For those asteroids from which UBV photometry is available (65 of 118), the Bus-DeMeo B-class objects with $(U–B) < 0.30$ and $(B–V) < 0.66$ were subsequently reclassified as being consistent with F class (33 total) and included in Table 2. The Tholen F-class asteroids with $(U–B) > 0.30$ do not satisfy our measurements for 2008 TC_3 and Almahata Sitta and were omitted. Similarly, Cb-class objects that plot in the Tholen B-class field of Fig. 5 were omitted (11 asteroids). That leaves a number of Bus Cb- and B-class objects with no certain Tholen classification. The SMASS optical spectra were examined to determine whether or not the blue part of the spectrum was sufficiently flat, with $(B–V) < 0.66$, and the near-IR slope not too red (1% increase max from 550 to 800 nm).

Ungrouped Asteroids

Figure 8 shows the distribution of these F- and B-class asteroids in the Main Belt. A total of 71 asteroids are classified as F class (listed in Table 2) and 32 classified as B class (not included in Table 2). They

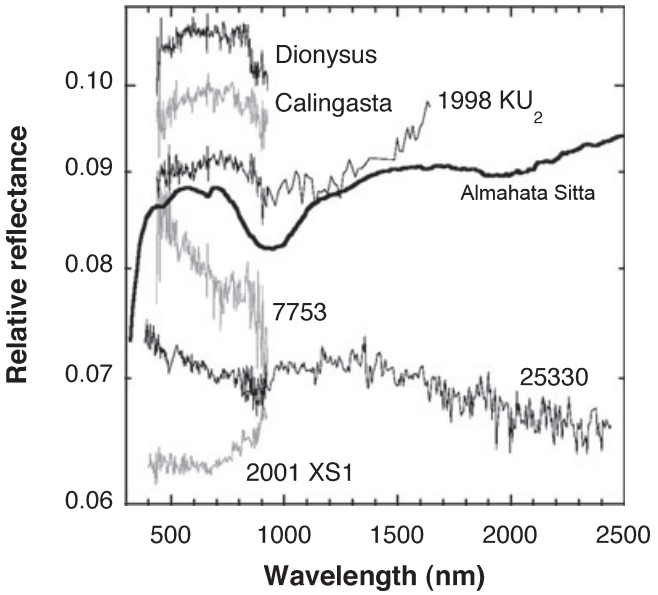

Fig. 5. The astronomical reflectance spectra of low-inclination $i < 20°$ NEA of F class (Table 1). Of these, the system of Bus (1999) classifies Dionysus and Calingasta as Cb and 7753 as a B class. Asteroid 25330 is a Ch class in the system of DeMeo et al. (2009). The spectra in this and the next figures are compared to the composite spectrum of Almahata Sitta shown in Fig. 2. Data were taken from the Planetary Data System's Asteroid/Dust Archive (Small Solar System Objects Spectroscopic Survey) and the Small Main Belt Asteroid Spectroscopic Survey SMASS (Binzel et al. 2010b).

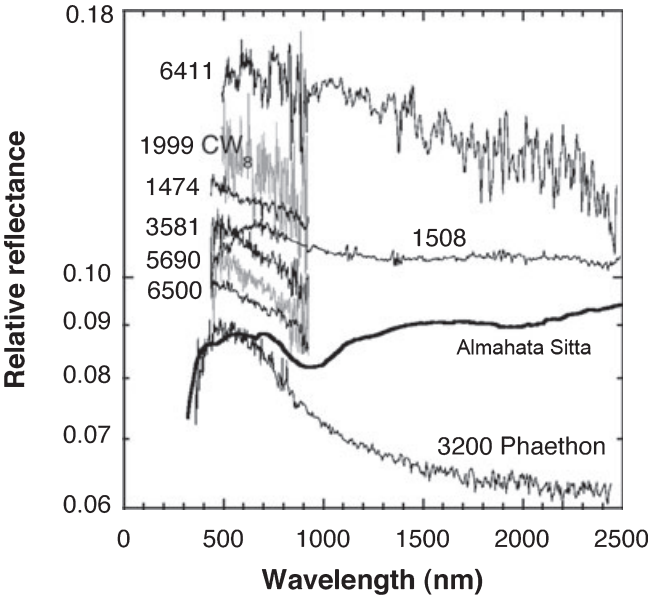

Fig. 6. As Fig. 5, now showing the astronomical reflectance spectra of high-inclination ($i > 20°$) NEA of F class (Table 1). The spectrum of 6411 Tamaga is from Clark et al. (2010).

include some of the largest known asteroids. Some have such a large size (e.g., 704 Interamnia at 317 km diameter) that they cannot all have originated from the same UPB, if that body had a diameter < 200 km.

The divergence of F-class objects becomes apparent when the spectral coverage is extended into the near-IR. Recently, Clark et al. (2010) published a number of different (F- and) B-class spectra; those that are F class in the Tholen taxonomy are reproduced in Fig. 9. A new spectrum for 142 Polana is also shown. These spectra were obtained with the IRTF SPeX instrument (Rayner et al. 2003). Most have a broad minimum in the 900–1500 nm range, but at various positions. The size and shape of the minimum do not appear to be related to the steepness of the visual or red slopes. The broad minimum around 1000 nm, seen in some B-class spectra and in the spectrum of 704 Interamnia, was recently ascribed to magnetite by Yang and Jewitt (2010).

The variety of F-class objects manifests also in other ways. 419 Aurelia has an unusual negative polarization branch, similar to 302 Clarissa and 704 Interamnia (Belskaya et al. 2005). 762 Pulcova, on the other hand, has normal polarization properties, so that this is not a common property of all F-class asteroids (for a more in-depth discussion, see Clark et al. 2010).

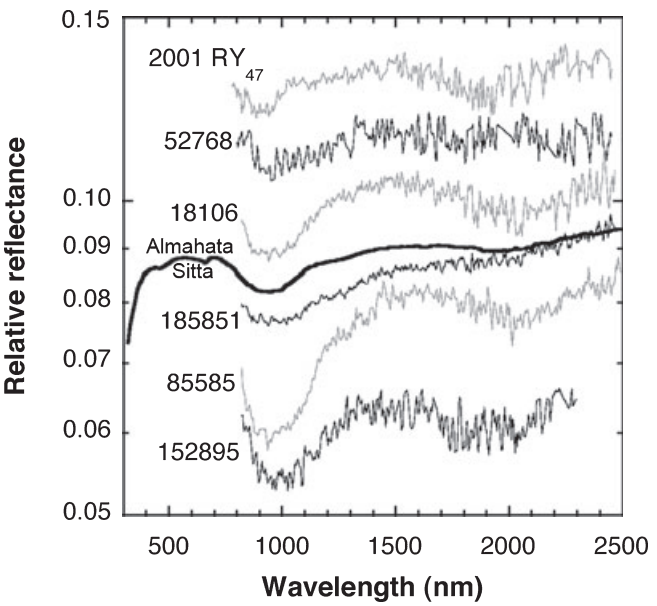

Fig. 7. New astronomical reflectance spectra of 2010a, NEA with spectra similar to Almahata Sitta (Table 1).

As mentioned before, it also remains to be seen which of the scattered F-class asteroids in the Main Belt are dry (Jones et al. 1990; Gaffey et al. 1993).

A Population of Scattered F-Class Asteroids

We do not expect the contemporary body that reaccreted from the UPB to be an isolated large

Table 2. Main Belt asteroids with F-class spectra.

Members	a[a] (AU)	e[a]	i[a] (°)	H (mag.)	D (km)	Albedo[b]	Class Tholen	Class DeMeo	Class This study
Hoffmeister family (F, low albedo)									
1726 Hoffmeister	2.787	0.047	4.379	12.1	26	0.037	–	Cb	F3
2930 Euripides	2.780	0.046	4.341	12.4	20	0.049	–	C	F3
4124 Herriot	2.787	0.048	4.373	12.5	20	0.045	–	B	F3
5091 Isakovskij	2.783	0.047	4.347	12.0	26	(0.040)	–	C	F3
5591 Koyo	2.780	0.049	4.347	12.5	21	(0.040)	–	Cb	F3
5866 Sachsen	2.790	0.047	4.370	13.8	12	(0.040)	–	–	–
6230 (1984 SG1)	2.788	0.047	4.370	13.1	16	(0.040)	–	C	F3
6716 (1990 RO1)	2.791	0.047	4.296	13.0	17	(0.040)	–	C	F3
6782 (1990 SU10)	2.790	0.046	4.410	12.5	21	(0.040)	–	Cb	F3
9920 (1981 EZ10)	2.784	0.047	4.347	13.6	15	0.027	–	–	–
Pallas family (F, high albedo)									
2 Pallas	2.771	0.281	33.199	3.9	532	0.159	B	B	Fp
531 Zerlina	2.786	0.255	33.055	11.8	15	0.146	–	B	Fp
2382 Nonie	2.760	0.275	32.950	11.4	17	(0.17)	–	B	B
3579 Rockholt	2.734	0.283	33.089	14.2	5	(0.17)	–	B	B
4997 Ksana	2.869	0.253	33.213	11.9	13	(0.17)	–	B	Fp
5222 Loffe	2.775	0.277	32.689	11.0	22	0.146	–	B	B
5234 Sechenov	2.761	0.272	33.123	11.4	17	(0.17)	–	B	B
5330 Senrikyu	2.764	0.262	31.848	11.8	12	0.223	–	B	B
Polana family (F, low albedo)									
142 Polana	2.418	0.158	3.216	10.3	55	0.045	F	B	F
302 Clarissa	2.406	0.106	3.346	10.9	39	0.052	F	B	F
750 Oskar	2.443	0.163	3.143	12.1	21	0.059	F	–	F
969 Leocadia	2.463	0.172	3.423	12.6	20	0.043	FXU:	–	F
1012 Sarema	2.479	0.155	3.231	12.4	21	0.043	F	–	F
1650 Heckmann	2.436	0.169	3.126	11.6	29	0.050	F	–	F
1740 Paavo Nurmi	2.467	0.155	3.061	13.2	13	(0.052)	F	–	F
2007 McCuskey[c]	2.384	0.150	2.850	11.8	22	0.070	–	–	F
2081 Sazava	2.450	0.152	3.073	12.1	23	0.048	F	–	F
2139 Makharadze	2.461	0.160	3.207	12.8	16	(0.052)	F	–	F
2278 Gotz	2.452	0.159	3.486	13.6	11	(0.052)	FC	–	F
2279 Barto	2.460	0.187	2.415	13.0	16	0.048	F	–	F
2527 Gregory	2.466	0.149	2.846	13.0	14	(0.052)	–	B	F
2809 Vernadskij	2.428	0.143	2.621	13.6	11	(0.052)	BFX	B	F
3130 Hillary[c]	2.466	0.160	3.284	12.8	16	(0.052)	–	–	F
3566 Levitan	2.361	0.158	3.042	12.8	16	(0.052)	–	B	F
4396 Gressmann	2.212	0.152	3.341	13.9	10	(0.052)	–	B	F
Nysa-like spectral shapes									
44 Nysa	2.423	0.174	3.059	6.9	71	0.546	E	Xc	Fn
877 Walkure	2.487	0.116	3.456	10.7	38	0.062	F	C	Fn:
1076 Viola	2.475	0.152	2.940	12.3	23	0.042	F	C	Fn
1493 Sigrid	2.430	0.168	3.100	12.0	24	0.049	F	Xc	Fn
1768 Appenzella	2.450	0.155	3.172	12.7	21	0.034	F	C	Fn
3192 A'Hearn	2.377	0.207	2.191	13.7	12	(0.042)	–	C	Fn
Theobalda family (F, low albedo)									
778 Theobalda	3.180	0.259	14.448	9.5	64	0.059	F	–	F
3432 Kobuchizawa	3.162	0.263	14.052	11.5	27	(0.059)	–	–	–
10982 Poerink	3.166	0.267	14.194	13.6	10	(0.059)	–	–	–
152549 (1119 T-3)	3.182	0.263	14.129	14.8	6	(0.059)	–	–	–
Themis family (B, low albedo)									
24 Themis	3.135	0.153	1.085	7.1	198	0.067	C	B	B
555 Norma	3.168	0.186	1.684	10.6	40	0.063	–	B	F
767 Bondia	3.118	0.154	1.367	10.0	42	0.102	–	B	F
2659 Millis	3.123	0.131	1.276	11.7	26	0.055	–	B	F

Table 2. *Continued*. Main Belt asteroids with F-class spectra.

Members	a[a] (AU)	e[a]	i[a] (°)	H (mag.)	D (km)	Albedo[b]	Class Tholen	Class DeMeo	Class This study
Ungrouped Main Belt asteroids with spectra similar to 2008 TC_3 at 435–925 nm (F)									
335 Roberta[d]	2.475	0.163	4.642	9.0	89	0.058	FP	B	F3
1277 Dolores	2.699	0.231	7.901	11.1	28	0.088	C	Cb	F3
2762 Fowler	2.331	0.191	5.329	13.2	12	(0.068)	–	Cb	F3
2772 Dugan	2.314	0.227	9.282	13.4	11	(0.068)	–	B	F3
2778 Tangshan	2.281	0.089	3.908	13.0	13	(0.068)	–	Cb	F3
2952 Lilliputia	2.314	0.152	3.883	14.1	9	0.051	–	Cb	F3
4194 Sweitzer	2.698	0.089	7.078	12.0	18	0.082	–	Cb	F3
4534 Rimskij-Korsakov	2.800	0.185	8.303	12.3	18	(0.068)	–	Cb	F3
4686 Maisica	2.365	0.118	5.389	13.4	11	(0.068)	–	B	F3
4944 Kozlovskij	2.744	0.026	5.611	12.8	14	(0.068)	–	Cb	F3
5079 Brubeck	2.641	0.237	12.386	12.6	17	0.059	–	B	F3
5329 Decaro	2.608	0.229	13.382	12.4	17	(0.068)	–	Cb	F3
5344 Ryabov	2.703	0.131	6.936	13.3	11	(0.068)	–	B	F3
7404 (1988 AA_5)	2.794	0.254	6.372	13.5	14	(0.068)	–	Cb	F3
9970 (1992 ST_1)	2.793	0.202	8.223	12.4	12	(0.068)	–	Cb	F3
Other ungrouped (F)									
85 Io	2.654	0.151	12.634	7.6	155	0.067	FC	B	F
210 Isabella	2.722	0.096	4.776	9.3	87	0.044	CF	Cb	F
213 Lilaea	2.753	0.145	5.769	8.6	83	0.090	F	B	F
225 Henrietta	3.376	0.212	22.786	8.7	120	0.040	F	–	F
282 Clorinde	2.339	0.103	8.823	10.9	39	0.050	BFU:	B	F
419 Aurelia	2.594	0.282	4.674	8.4	129	0.046	F	–	F
438 Zeuxo	2.554	0.077	6.525	9.8	61	0.057	F:	–	F
545 Messalina	3.184	0.181	11.753	8.8	111	0.042	CD	Cb	F
704 Interamnia	3.061	0.104	18.785	5.9	317	0.074	F	B	F
762 Pulcova	3.157	0.128	13.919	8.3	137	0.046	F	–	F
880 Herba	3.002	0.256	17.933	11.5	–	–	F	–	F
1021 Flammario	2.738	0.246	15.741	9.0	99	0.046	F	B	F
1080 Orchis	2.418	0.244	4.941	12.2	23	0.043	F	–	F
1111 Reinmuthia	2.994	0.064	2.993	10.7	–	–	FXU:	–	F
1154 Astronomia	3.394	0.070	2.993	10.5	61	0.030	FXU:	–	F
1484 Postrema	2.738	0.239	16.501	12.1	43	0.014	–	B	F
1579 Herrick	3.427	0.138	9.036	10.7	43	0.052	F	–	F
1655 Comas Sola	2.783	0.223	8.296	11.0	31	0.073	XFU	B	F
1705 Tapio	2.299	0.195	7.765	12.8	11	0.118	–	B	F
1796 Riga	3.356	0.097	22.350	9.8	74	0.038	XFCU	Cb	F
2251 Tikhov	2.711	0.106	7.517	11.4	26	0.070	–	Cb	F
2370 van Altena	2.714	0.150	8.191	12.6	13	0.090	–	Cb	F
2816 Pien	2.727	0.145	6.777	11.7	22	0.077	–	B	F
3123 Dunham	2.462	0.102	1.279	13.5	–	–	F	–	F
3627 Sayers	2.349	0.180	8.982	13.2	–	–	–	B	F
3647 Dermott	2.800	0.067	7.037	11.4	31	0.052	–	B	F
4297 Eichhorn	2.355	0.163	4.955	12.7	–	–	–	Cb	F
5102 Benfranklin	2.800	0.153	9.122	12.7	18	0.044	–	B	F
5133 Phillipadams	2.713	0.182	11.354	11.5	25	0.070	–	B	F

[a]Proper orbital elements (mean over 1 Myr of integration).
[b]Between brackets are assumed albedos (based on other family members) used for the calculation of asteroid diameters (Migliorini et al. 1996).
[c]Added, based on spectroscopy by Manara et al. (2001).
[d]Possible member of Polana family.
":" means uncertain.

asteroid at the present time. Although 2008 TC_3 could be a chip from any of these isolated asteroids, it is difficult to argue why all ureilites should derive from any particular single asteroid. Even if these isolated asteroids contribute to an influx of ureilites, it is statistically more likely that 2008 TC_3 originated from

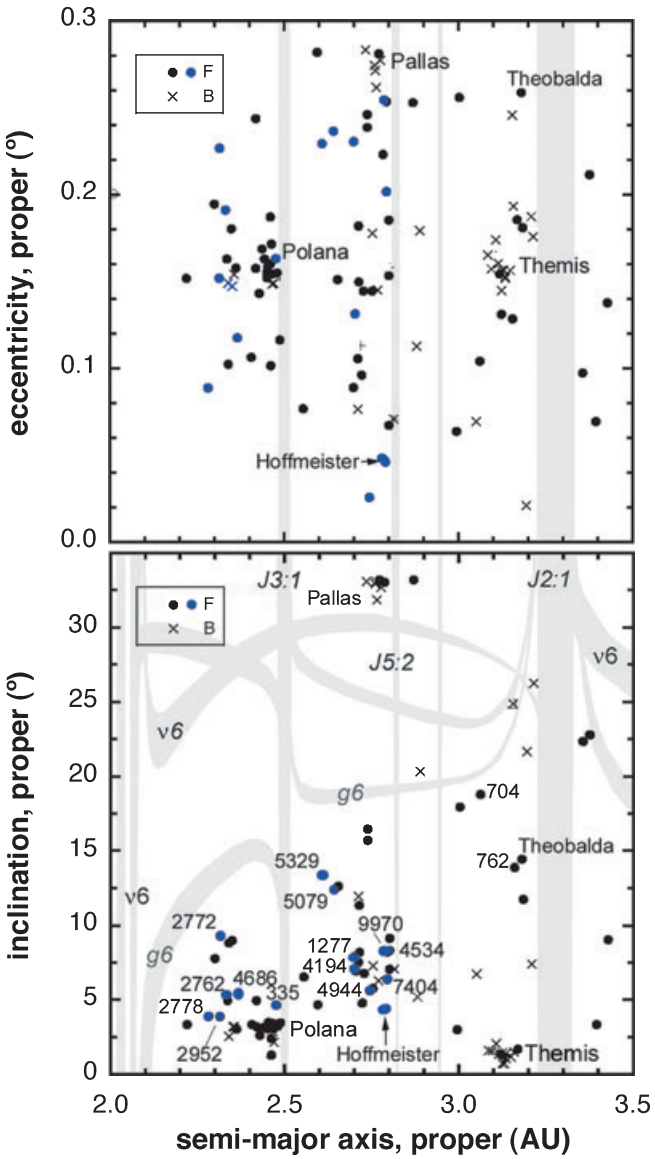

Fig. 8. Location of F- and B-class asteroids in the Main Belt, with blue colors marking the objects for which SMASS data are available that have reflectance spectra most like 2008 TC_3. F-class asteroids are concentrated in the Polana, Pallas, Hoffmeister, and Theobalda families. Resonances (gray) are from Knezevic et al. (1991).

an F-class asteroid family, which have a much larger combined cross sectional area for collisions.

The question remains whether or not these ungrouped objects are related. If they are, then this population of scattered F-class asteroids could be a source for 2008 TC_3. Only eight of the ungrouped F-class asteroids are larger than 100 km in diameter (4% of the known Main Belt asteroids larger than 100 km). Asteroids <100 km in diameter are thought to be collisional products from a fragmentation in the past (Bottke et al. 2005a, 2005b; Morbidelli et al. 2009).

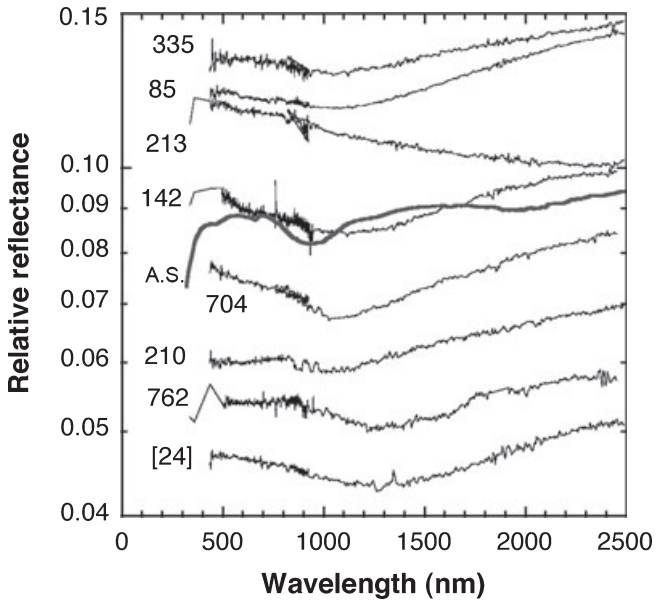

Fig. 9. New near-infrared (IR) reflectance spectra of ungrouped Main Belt asteroids of F class (some previously discussed in Clark et al. 2010). When the spectra are extended into the near-IR wavelength range, a divergence in properties is seen. Within the full visible to near-IR taxonomy system of DeMeo et al. (2009), most are classified as Cb (142, 210, 704) or C (85, 762), whereas Pallas is classified as B type. Also shown is that of B-class 24 Themis. The optical spectra were obtained by the SMASS program.

Indeed, some 13 of 59 ungrouped F-class asteroid reflectance spectra have about the same slope in the 435–925 nm SMASS spectra (Fig. 10), albeit with what appears to be a 50% (on average) weaker pyroxene band. These are listed separately in Table 2. These potential kin of 2008 TC_3 are distributed throughout the inner and central belt, just inside of the 3:1 and 5:2 resonances, respectively (blue dots in Fig. 8), but are not found in the outer belt. This orbital distribution is consistent with the source regions for 2008 TC_3 predicted above.

There are no statistically significant differences between the spectra of the inner and central Main Belt objects. Albedos for these objects are in the range of 0.059–0.088. The spectra are plotted in Fig. 10. They have a 435–925 nm slope similar, meaning that the least-squares fit linear slope of the relative reflectance normalized to 1.0 at 500 nm is in range of −8.3 to -3.7×10^{-5} nm^{-1}, to 2008 TC_3 (-6.7×10^{-5} nm^{-1}). Asteroid 85 Io was excluded, because it did not exhibit the pyroxene band. Two spectra with a slightly red slope, asteroids 1277 and 4944, are also included as their slightly stronger downward curvature toward shorter wavelengths (responsible for the red slope) is also a reasonable fit to the Almahata Sitta composite (Fig. 10).

The large 335 Roberta is a suspected member of the Polana family (see below), but in detail has a different

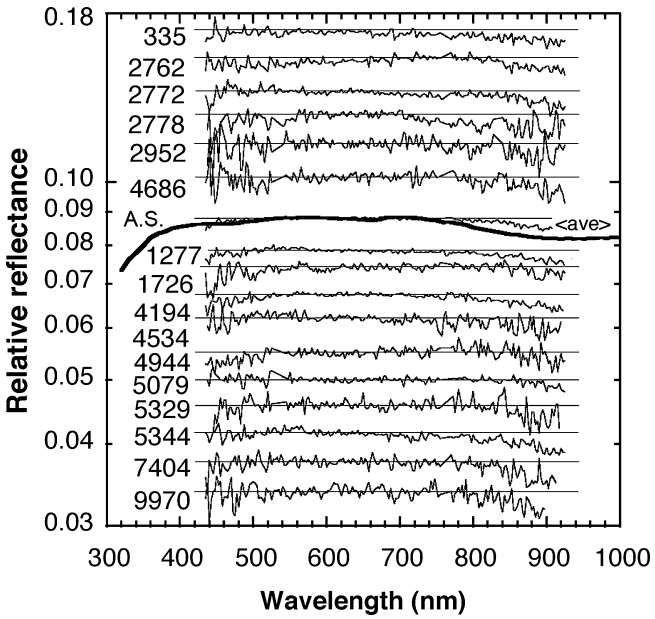

Fig. 10. Ungrouped asteroids in the inner Main Belt (top) and the central Main Belt (bottom) with SMASS reflectance spectra most like 2008 TC_3. Also shown is 1726 Hoffmeister, part of the Hoffmeister family. Solid lines are placed to match the central part of the reflectance, showing the depth of the 900 nm pyroxene band. "< ave >" is the average of all spectra.

spectrum than 142 Polana (Fig. 9). Most other asteroids have diameters in the range of 10–20 km (Table 2).

The Theobalda Family

Each of these stray asteroids can flag the nearby presence of a family of F-class asteroids, smaller members of which may not yet have been classified. For that reason, we studied the distribution of known asteroids in proper element space near each of these strays in search of families. We recovered only one such case, associated with 778 Theobalda in the vicinity of the J2:1 mean-motion resonance (Fig. 11), a previously known family (Zappalà et al. 1997). Because Theobalda is an F class, the nearby asteroids in the Theobalda family might be also.

Theobalda itself is 67 km in diameter, whereas all other members are much smaller, making this an apparent cratering family, which is a family of asteroids from an impact that did not disrupt the parent body itself (Durda et al. 2007). Novakovic (2010) recently counted 128 members and determined an age of only 6.9 ± 2.3 Myr and an original parent body size of 78 ± 9 km. This makes the family too young to account for the CRE age of Almahata Sitta. Moreover, 778 Theobalda has a slightly red-sloped SMASS optical reflection spectrum, with no sign of a pyroxene band (not shown).

The Hoffmeister Family

The small Hoffmeister family in the central Main Belt (Fig. 12) has no large representative body, suggesting that it is the product of a supercatastrophic collision (Durda et al. 2007). The family consists of a series of relatively small 10–20 km-sized asteroids. Namesake 1726 Hoffmeister is at 26 km diameter barely larger than others. Migliorini et al. (1996) estimated that the original body had a diameter of D = 50–100 km (summing the volume of known asteroids gives D = 69 km). By modeling the breakup of the Hoffmeister family, Durda et al. (2007) put the original body at D = 136 ± 6 km, because as much as 90% of the mass is unaccounted for in fragments smaller than 9 km. The best fit to the Hoffmeister family size distribution was obtained with a 7 km s^{-1} impact of a 51 km-sized asteroid hitting a basalt target at a 45° impact angle. The group is tight (Fig. 12) with a small spread in the three proper orbital elements indicative of relative speeds following the breakup of less than a few tens of m s^{-1} (Migliorini et al. 1996). The age of the cluster was determined at 300 ± 200 Myr (Nesvorný et al. 2005). IRAS albedos of three family members are in the range of 0.037–0.069 (Tedesco 1994). 4516 Pugovkin and 2996 Bowman, thought to be Hoffmeister family members, have distinctly different spectra, classified as Sl and Xc, respectively, and may be interlopers.

Several family members have optical spectra similar to 2008 TC_3, including a weak downturn at the longest wavelengths (Fig. 13). As with the ungrouped asteroids mentioned before, the band appears to be a pyroxene band with a depth of only approximately 50% of that in 2008 TC_3. However, on extending the spectrum into the near-IR, the match with 2008 TC_3 breaks down (Fig. 13). The downturn is the onset of a broad depression centered on 1400 nm, not seen in 2008 TC_3.

The Polana Family

The prominent cluster in (a, e, i) proper element space at $a \sim 2.4$ AU ($e \sim 0.16$; Fig. 11) has been called various names: the Nysa family, Nysa-Herta family, and the Nysa-Polana family (Burbine et al. 2002; Mothé-Diniz et al. 2005). Cellino et al. (2001) inferred that the cluster actually consisted of two distinct groupings that overlap in proper element orbital space. One group of objects, consisting of dark asteroids including several F-class members, they named after its least-numbered member, 142 Polana. The second group of S-class asteroids was named after the most plausible least-numbered member, 878 Mildred. The two largest asteroids, 44 Nysa (E class) and 135 Herta (M class), appear to be interlopers.

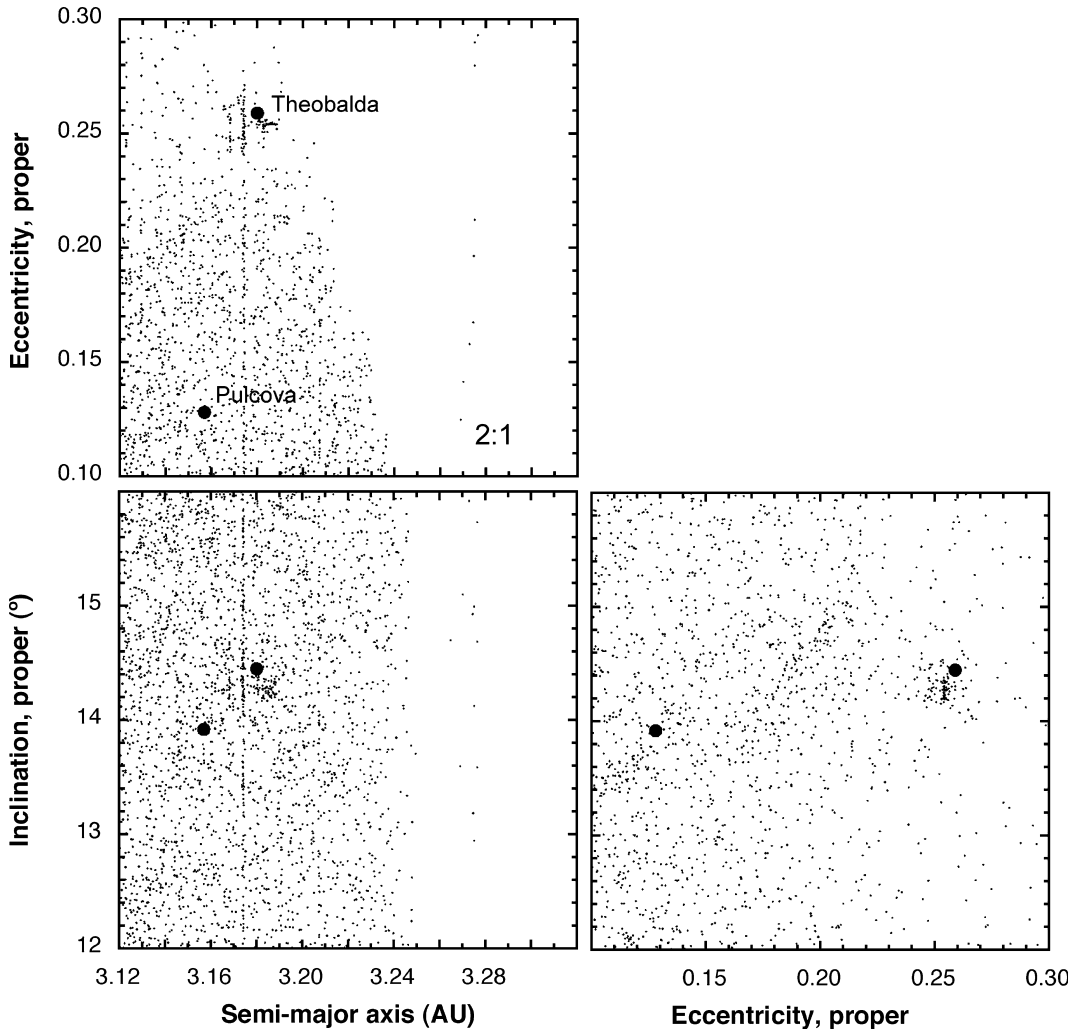

Fig. 11. Distribution of proper elements in the vicinity of F-class asteroids 762 Pulcova and 778 Theobalda. Only the objects shown in the bottom left diagram are included in the top and right diagrams. Note the Theobalda cratering family.

The Polana family has many known members. At the present time, the Polana-Mildred family has the third largest number of known members, after the Vesta and Flora families, despite the relatively low albedo of its members (Nesvorný et al. 2006a). Twenty-two of 61 F-class asteroids in Table 2 with inclination $i < 10°$ are Polana family members. Most are relatively small, however, so that the high count could be because the family is in the inner Main Belt, and therefore on average closer to Earth than the previous families. The sum of all members does not add up to a particularly large initial object. Taken together, all identified members listed in Table 2 (and those shown in Fig. 14) would make an asteroid of approximately 86 km in diameter, assuming an albedo of 0.046 and mean density of 2.0 g cm^{-3}. 142 Polana, at 55 km, accounts for approximately 40% of the mass of known family members, making this a barely catastrophic collision (Durda et al. 2007).

In recent years, so many asteroids have been discovered that it has become possible to recognize the outline of both the Polana and Mildred groups in the distribution of asteroids in proper element *a–e* and *a–i* diagrams (Fig. 14). We used the SLOAN digital sky survey colors of the asteroids selected by Zappalà et al. (1995) to distinguish the Polana family from the Mildred family (Juric et al. 2002). The Mildred family (+) makes the densest cluster, whereas the Polana family (•) is more diffuse and slightly offset, adjacent to the J3:1 mean-motion resonance. Most known F-class members of the Polana group (large light blue dots, the larger members in the family) are outside the *a–i* contour of the densest concentration of asteroids. Objects scatter along a diffuse ridge in the *e–i* diagram. The core of the F-class family is at slightly lower proper inclination $i = 2.5°$ than most objects identified so far. This implies that the Polana family continues into the background. Indeed, several

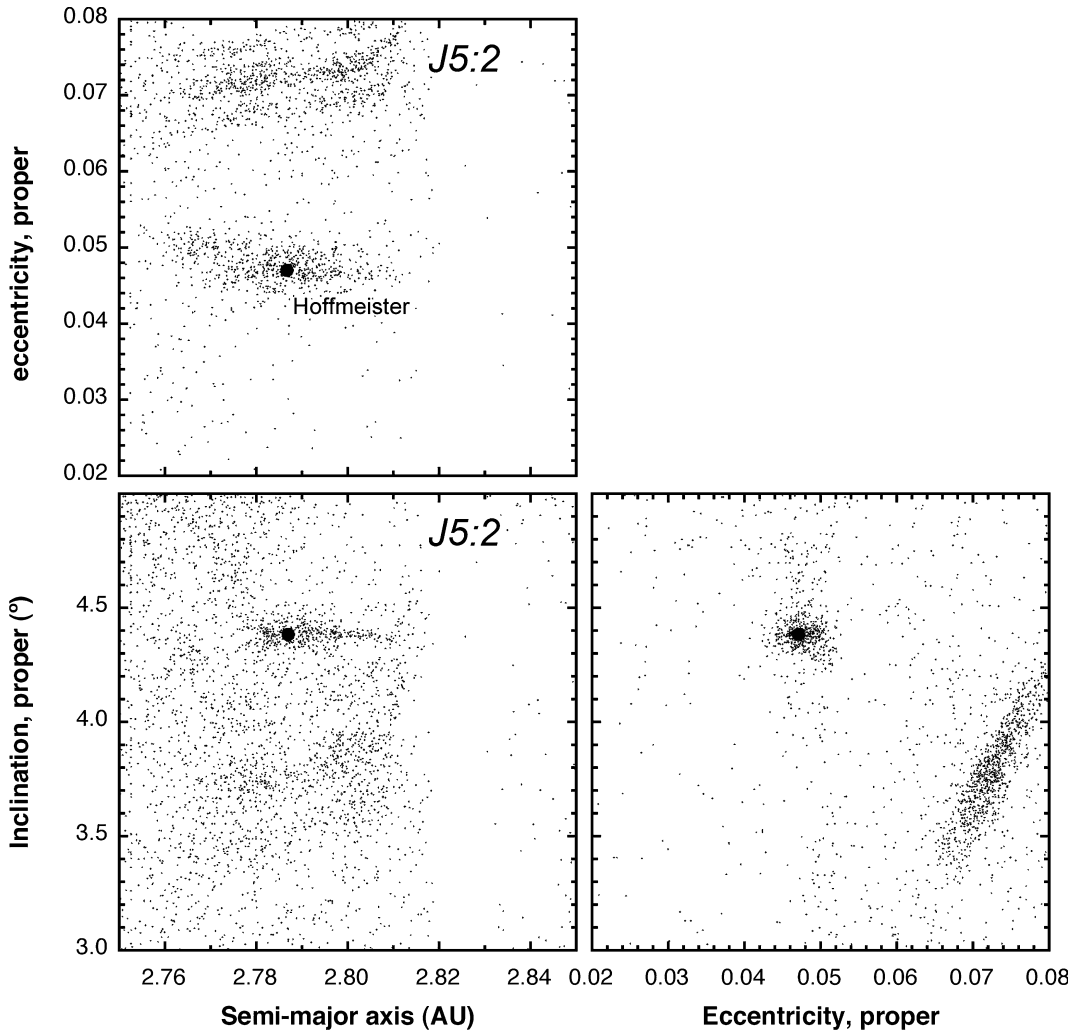

Fig. 12. Distribution of proper elements in the vicinity of asteroid 1726 Hoffmeister (•). Note how many of the detected Hoffmeister family members have evolved toward the J5:2 mean-motion resonance.

stray F-class asteroids in the inner Main Belt (Fig. 11) may belong to this family.

The size distribution of the thus selected Polana family members suggests that mass is about equally distributed among log (mass) interval bins. If the observed mass distribution is extrapolated to sizes as small as 2008 TC_3, then the initial parent body diameter would have been about 117 ± 9 km. If 44 Nysa was part of the original body as well, then Nysa would represent about one-third of the original mass of 1.0×10^{18} kg. The original diameter in that case is approximately 137 km.

Polana and most family members have a reflectance spectrum with a weak pyroxene band like 2008 TC_3, but with a blue slope < 600 nm (Fig. 9). Other family members have optical spectra not unlike that of 44 Nysa, but a much lower albedo (Fig. 15). They have a reddish slope below 700 nm unlike 2008 TC_3.

Nysa (Fig. 16), with a spectrum similar to enstatite chondrite meteorites, is found in between the Polana and the Mildred family, at the tip of a string of Polana family members (Fig. 14). It was earlier proposed that 44 Nysa was the inner portion (core) of the original protoplanet that gave rise to the Polana family (Tedesco et al. 1982a). Unlike these other members, Nysa has an unusually high albedo of 0.55. Some color variation on the surface has been detected (Tupieva 2003; Rosenbush et al. 2009). Also, Nysa has a strong 3 μm absorption band, which requires about 2–5 wt% H_2O/OH if it were in volatile-rich meteorites (Britt et al. 1994).

The relationship, if any, with the Mildred family is unclear. Mildred family optical reflectance spectra have been studied by Mothé-Diniz et al. (2005). Near-IR SMASSII survey spectra exist for only a few core members in *e–i* diagram: 1932 Jansky (Sl), 2818 Juvenalls (S), and 4817 (1984 DC1) (Sl). All spectra

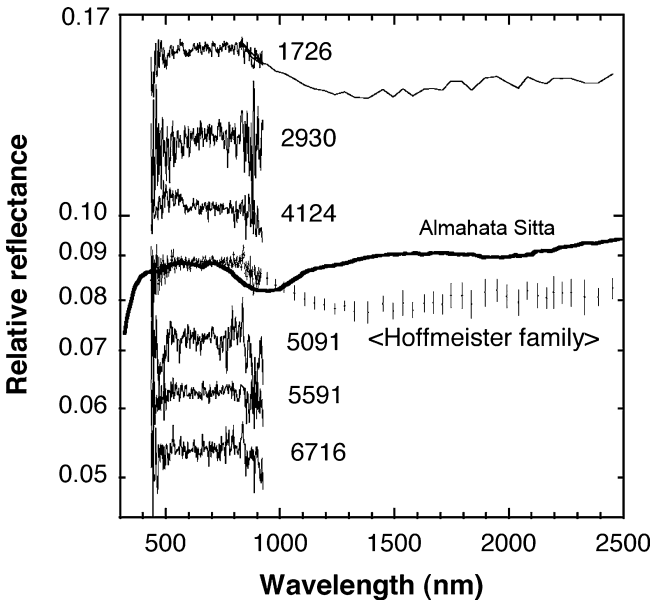

Fig. 13. Reflectance spectrum of Hoffmeister family members from the SMASS (Binzel et al. 2010a, 2010b), and a new near-IR spectrum of asteroid 1726 Hoffmeister. Spectra are displaced for clarity. "<Hoffmeister family>" is the average spectrum of all available data.

have the same steep visible slope and a deep pyroxene band as the spectrum of 2818 Juvenalis shown in Fig. 17. The middle cluster in the *e–i* diagram has measured candidates: 3654 AAS (Sq) and 5318 Dientzenhofer (Sk) with significantly different spectral shape, possibly a mix of S and F (not shown).

M-class 135 Hertha is found in between the Mildred and Polana families (Fig. 14), with a reflectance spectrum (Fig. 16) that shows a weak 900 nm feature from ortho-pyroxenes not seen in other M-class asteroids (Kelley et al. 1994). Radar observations show that the surface is not metallic (Shepard et al. 2008, 2009). From that, it was concluded that 135 Herta is not a metallic core from a differentiated asteroid, but rather composed of silicate material. Rivkin et al. (1995, 2000) argued Herta might be of W class.

The Pallas Family

Asteroid 2 Pallas ($291 \times 278 \times 250$ km) is often classified as B class, but would fall in our F-class domain in Fig. 3. 2 Pallas has a weak 3 μm feature from hydrated silicates not seen in the Almahata Sitta meteorites (Lebofsky 1980; Rivkin et al. 1996, 2002). It has a reflectance spectrum that continues to decrease at wavelengths above 900 nm (Fig. 17).

All family members with known visible spectra have a slightly bluish slope (Fig. 17). The shape of these reflectance spectra straddle the F and B domains, some here are classified as B class, others as F class (Table 2). All appear to have a weak pyroxene band. 2 Pallas itself is much larger than its family members, suggesting that this is a cratering family. Indeed, Pallas is known to have a large impact crater on the southern hemisphere (Schmidt et al. 2009).

The Themis Family

Members of the Themis family in the outer Main Belt (Fig. 8) classify mostly as B class, as does 24 Themis itself (Fig. 9). Most Themis family members have an absorption band at 700 nm, not seen in 2008 TC_3. The large 198 km-sized 24 Themis contains a 3 μm absorption band (Jones et al. 1990; Lebofsky et al. 1990), perhaps with a shape indicative of water ice (Campins et al. 2010; but see Clark et al. 2010). Only for the sake of completeness, those that classify as F are listed in Table 2. The spectra of Themis family members differ from 2008 TC_3, in a manner that cannot be ascribed to more space weathering or a regolith at the surface.

DISCUSSION

Dynamical Arguments

The presence of kilometer-sized NEA with spectra similar to 2008 TC_3 is consistent with a source region of both small (meter-sized) and larger (kilometer-sized) ureilitic objects in the Main Belt. Locations adjacent to the ν_6 secular resonance and inner Main Belt Mars- and three-body resonances (IMC) are the most likely source region of 2008 TC_3 according to the statistical model by Bottke et al. (2002b), but the asteroid could also have originated from the J3:1 resonance. If 1998 KU_2 and others originated from the same debris field as 2008 TC_3, only more recently perhaps, then we are no longer only looking at objects bleeding from the ν_6 and IMC resonances. The probability of 1998 KU_2 coming from the ν_6, IMC, J3:1, and outer Main Belt mean-motion resonances is 41%, 32%, 23%, and 4%, respectively. Hence, nearly all potential source families have a reasonable probability of producing this object. Of other members in this group (Table 1), asteroid 85585 is most likely to come from the J3:1, others from the ν_6, some from the IMC region.

The CRE age of 2008 TC_3 suggests that the parent asteroid was located fairly close to a mean-motion resonance. If the spin on 2008 TC_3 dates from this impact, then the Yarkovsky effect can be calculated (Vokrouhlicky et al. 2006). Using a 49 s spinning period, 4 m-sized object, ureilite material, and a thermal conductivity consistent with bare rock, we estimate that 2008 TC_3 would drift 0.02–0.03 AU for 0/180° obliquity

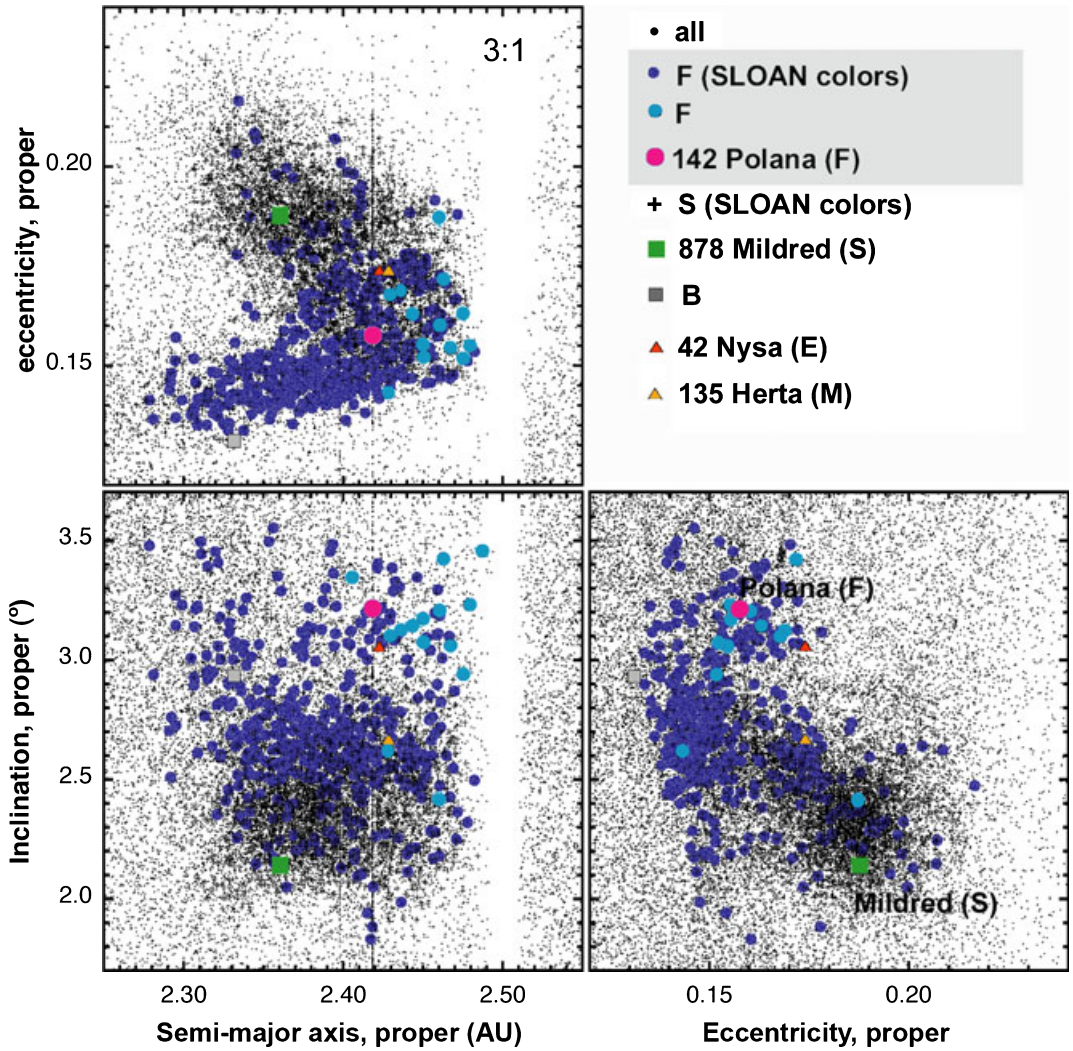

Fig. 14. Distribution of asteroids in proper orbital element space in the neighborhood of the Polana family (all asteroids with F-class Sloan colors are shown by blue •) and the Mildred family (all S-class asteroids shown by a small black +). Large light blue symbols mark members that were classified as F class. Synthetic proper orbital elements were derived from the Astdys database, calculated by Novakovic, Knezevic, and Milani (July 2009). Asteroids that plotted in the lower left graph were replotted using different orbital elements in the plots above and to the right. Possible interlopers Nysa and Herta are shown as filled triangles.

over this time scale. This means that the parent asteroid is expected to be <0.03 AU from a mean-motion resonance efficient in ejection meteoroids. If 2008 TC_3 somehow had a dusty surface, however, Yarkovsky semimajor axis drift forces would have been considerably more effective, such that the object could have come from a much great distance (e.g., Bottke et al. 2006).

The Pallas Family and the Origin of 3200 Phaethon

The Pallas family has a high inclination (~33°). Numerical simulations suggest that Main Belt asteroids with high inclinations, such as Pallas family members, that are evolving into the NEO region are unlikely to achieve 2008 TC_3-like low-inclination orbits. Taken together with the fact that 2 Pallas has a 3 μm signature, this probably excludes the Pallas family as a likely source for 2008 TC_3.

Instead, the Pallas family is likely responsible for the high-inclination group of F-class asteroids in Table 1 (Fig. 5). All but one, 1508 Kemi, have a blue-sloped visible spectrum, not unlike that of 2 Pallas. In this context, F-class NEA 3200 Phaethon (Fig. 3) is of particular interest, because it is the parent body of the Geminid meteor shower (e.g., Jenniskens 2006). Phaethon was earlier proposed to originate from the Polana family (Zappalà et al. 1994). Instead, Phaethon has a weak 3 μm absorption band similar to that of 2 Pallas. The near-IR spectrum is more steeply sloped than 2 Pallas (Fig. 17), possibly on account of surface

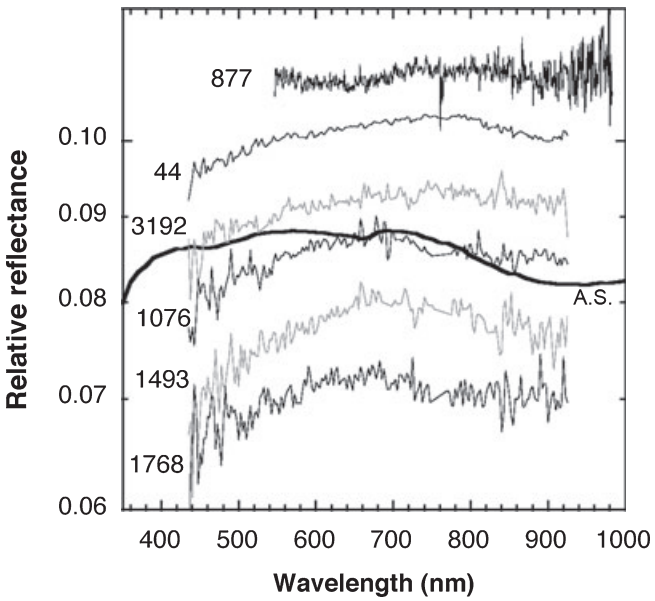

Fig. 15. Reflectance spectra of members of those Polana family members that have Nysa-like optical spectra (but much lower albedo). 44 Nysa is also shown. Data were taken from the Planetary Data System's Asteroid/Dust archive and were obtained by the Small Solar System Objects Spectroscopic Survey, and the SMASS and SMASSII (Binzel et al. 2010b).

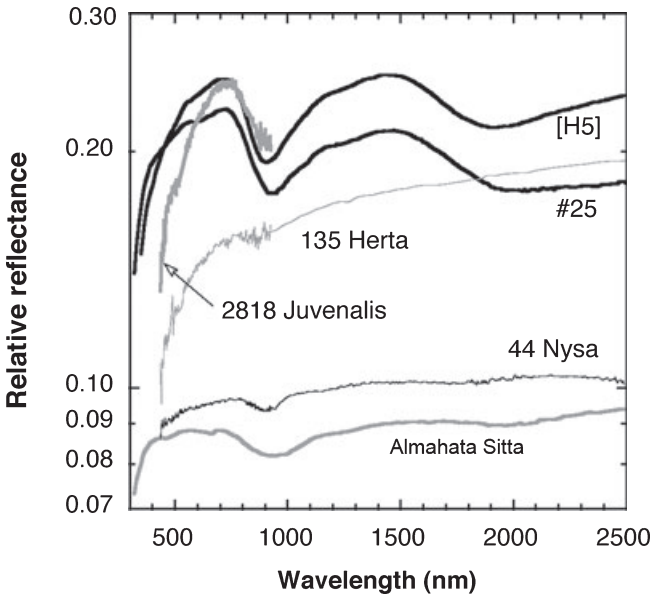

Fig. 16. Reflectance spectrum of Mildred family member 2818 Juvenalis (classified as S class). Member 1932 Janksy (not shown) has a very similar, but noisier, spectrum, possibly with a slightly weaker 1 μm band. The reflectance spectrum of Almahata Sitta sample #25 is compared to the meteorite type H5 mean spectrum by Gaffey et al. (1990), taken from the Planetary Data System's Asteroid/Dust archive. Also shown are the spectra of M-class 135 Herta (from Fornaisier et al. 2010) and E-class 44 Nysa (from Clark et al. 2004).

heating due to its small perihelion distance of $q = 0.14$ AU (Ohtsuka et al. 2009). In other aspects, there is good agreement between the spectrum of 3200 Phaethon and that of 2 Pallas, as was recently independently pointed out by DeLeón et al. (2010) and Campins et al. (2010). In addition, Campins et al. (2010) showed a plausible dynamical link between the Pallas family and Phaethon.

Interestingly, there is ample evidence of a progressive fragmentation of 3200 Phaethon, including not just the breakup event that created the Geminid meteoroid stream (Jenniskens 2006). Asteroid 2005 UD is the parent of the Sextantid shower (Ohtsuka 2005) and has the same spectral reflectance as Phaethon (Jewitt and Hsieh 2006; Kinoshita et al. 2007). It is found along the same secular nodal-line rotation cycle as Phaethon's (Jenniskens 2006). Hence, Phaethon and its family members must have low tensile strength and be composed of fine-grained material in a manner that breakup would generate a cloud of meteoroids, but it would be different material than the fragile Almahata Sitta ureilitic breccia, because Almahata Sitta lacks a 3 μm band. Clark et al. (2010) recently found a trend of analogs from the CV, CO, and CK meteorite types, instead.

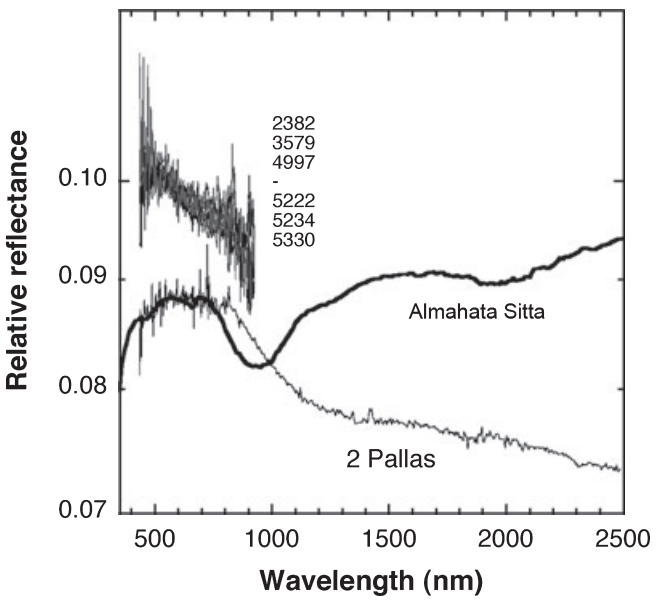

Fig. 17. Reflectance spectra of the Pallas family asteroids from the SMASS. Data for 2 Pallas are from Sawyer (1998) and the 52-color photometric survey. 2 Pallas itself is displaced for clarity.

Hoffmeister as a Source of Supercollision Fragments

Aside from the Theobalda family being too young, the family is too far from the J2:1 mean-motion resonance to be a likely source of the ureilites through that pathway. The family is located on top of the 5-2-2 three-body resonance near 3.17 AU, which is

responsible for the vertical line of asteroids in Fig. 11, but this is not an efficient delivery resonance for meteorites (Gladman et al. 1997; Bottke et al. 2006). All things being equal, families in the outer Main Belt have a low likelihood of producing numerous meteorites because the delivery efficiencies are very low (~0.01%) compared to objects in the innermost region of the Main Belt (~1%), and the central Main Belt (0.1–0.3%). Only in a supercatastrophic breakup can an asteroid family overcome these odds, when numerous small fragments are created (Durda et al. 2007).

The Hoffmeister family had such a case of supercatastrophic breakup. The smallest fragments evolved most quickly by the Yarkovsky effect to both the J5:2 and J3:1 resonances. Because the collision was relatively recent, this family is a potential source of ureilites, in the same way as the creation approximately 470 Ma of the Gefion family is a likely source of shocked L chondrites, one of the largest fraction of meteorite falls today (Nesvorný et al. 2009). The Gefion collision is thought to have generated many small fragments that quickly evolved into the J3:1 and J5:2 resonances, the J3:1 resonance being the likely supply mechanism. The Hoffmeister family shares many attributes of the Gefion family: (1) it is located 0.03 AU from the inner edge of the J5:2 mean-motion resonance, much like the Gefion family at $a \sim 2.79$ and $i \sim 9.1°$. A tail of asteroids shows that it is leaking material into the J5:2 resonance (Fig. 12); (2) the family is young (~300 versus 470 Myr, respectively); (3) both parents were similar in size; and (4) both families were produced by supercatastrophic disruption events that are capable of producing lots of smaller asteroids and meteoroid-size fragments.

Many things had to go right for the Gefion family fragments/L chondrites to dominate our meteoroid fall statistics. The biggest factor may be that small Gefion fragments have had time to drift down by the Yarkovsky effect to the J3:1 resonance, which is much better at meteoroid delivery to Earth than the J5:2 (Nesvorný et al. 2009). Because the Hoffmeister family is about 170 Myr younger than the Gefion family, the much lower rate of ureilite falls could be on account that many or perhaps most of the Hoffmeister fragments have not yet reached the J3:1 resonance. Possibly the advance guard of tiny fragments from the family forming event have already reached the J3:1, or perhaps the flux of meteoroids reaching the J5:2 by the Yarkovsky effect is so large that a few show up in our fall statistics. In both cases, 2008 TC_3 must have been the product of a collisional cascade that created the fragment from a larger asteroid close to either resonance.

On the other hand, 2008 TC_3 has an orbit that strongly suggests that it came from the inner asteroid belt and not from any resonance beyond 2.5 AU (J3:1, J5:2, etc.). The Bottke et al. (2002b) model predicts the probability that 2008 TC_3 came from the ν6 resonance, the large quantity of Mars- and three-body resonances in the inner Main Belt and the J3:1, 80% and 20%, respectively. Hence, odds are stacked against it as a source for 2008 TC_3. The dissimilarity between the near-IR spectra of 1726 Hoffmeister and Almahata Sitta (Fig. 14) also argues against the ureilites originating from this source.

If ureilites originated from the Hoffmeister family, it would have been fitting that the family was named after asteroid 1726 Hoffmeister, which in turn was named for Cuno Hoffmeister (1892–1968), a well-known German meteor astronomer, who wrote the 1937 book "Die Meteore" (Leipzig: Akademische Verlag) and the 1948 book "Meteorströme" (Leipzig: Barth Verlag).

Polana and Mildred: Evidence for the Catastrophic UPB Collision?

The same argument applies for the Polana family, with meteorite delivery through the ν_6 and J3:1 resonances that bracket both sides of the inner Main Belt. Polana also librates about the M2:1 resonance with Mars (Gallardo 2007). In this sense, there are similarities with the Vesta family asteroids thought to be responsible for V-class NEA and HED meteorites (e.g., Gaffey 1993; Migliorini et al. 1997; Moskovitz et al. 2008, 2010). The fact that ureilites are the most common type of achondrite following HED meteorites is consistent with the large size (and large surface area) of the Polana family members, even though we are unlikely to be getting a representative sample of what is being ejected. The Polana family is located in between the S-class rich inner belt and the C-class rich outer belt, the correct location for a UPB if rigid radial zoning of initial asteroid class existed (Cellino 2004).

The dynamical lifetime of the Polana family is unknown because the overlapping Mildred family makes such studies difficult (Vokrouhlicky et al. 2006), but is likely in excess of 500 Myr, and probably >1 Gy, given its relatively large dispersion in semimajor axis of identified members. The number of small objects in the Polana family is unknown. The large members are not significantly more numerous than those in the Hoffmeister family.

At typical impact speeds (~5 km s^{-1} in the asteroid belt), asteroids are catastrophically destroyed by projectiles having approximately 0.1% or less of the mass of the target (Bottke et al. 2002a). The residue of the impactor is rarely recognized, making most asteroid families of single taxonomic type. Could the Polana-Mildred family be an exception? Could the Polana and Mildred families be the product of a rare (read:

unlikely) collision of two relatively large asteroids? In that case, the mass ratio of impactor to impactee is about 0.15, with the total mass of known Mildred family asteroids (assuming albedo = 0.54 and density = 3.5 g cm^{-3}) estimated at 2.4×10^{16} kg (a 23 km diameter asteroid). Indeed, the probability of 23 km asteroid hitting an 86 (and even more so a 137) km diameter asteroid is negligible on the time scale of the solar system. The collisional lifetime for an 86 km asteroid in the present asteroid belt is about 30 Gy (Bottke et al. 2005a).

There are some suggestive hints, however, that the two families have a shared dynamical history. Most of that probably comes on account of Yarkovsky-drift of the smaller asteroids over the age of the cluster, combined with the influence of resonances in the region (e.g., Vokrouhlicky et al. 2006), not from a mutual collision. The bulk of smaller Polana family members is at lower inclination and has slightly lower eccentricity from the larger members of the Polana family, with most smaller Polana family members having the same inclination as the debris field of the S-class Mildred family. In the *e–i* diagram (Fig. 14, right diagram), a tail of debris is found between the S- and F-class clusters, with possibly a concentration near the center. In the *a–e* diagram (Fig. 14, top diagram), a tail of debris emanates from the F-class cluster, pointing toward lower values of semimajor axis. The direction of the tail is toward the lower semimajor axis of the S-class asteroids. If a mutual collision did occur, this could perhaps be interpreted to mean that in the collision, the debris that now comprises the Polana family members lost momentum. Without modeling of the collision event (e.g., Nesvorný et al. 2006b), this suggestion remains speculative.

With or without a mutual collision, the Mildred family could have added foreign clasts to the Polana family members on account of their similar orbits. To test the hypothesis that foreign clasts in Almahata Sitta could derive from the Mildred family, the Mildred family spectra are compared in Fig. 16 to the reflectance spectrum of Almahata Sitta #25 and an H5 chondrite mean spectrum by Gaffey et al. (1990). The Almahata Sitta clast, like other H5 chondrites, has a more gradual shoulder diving into the pyroxene band, similar to the Mildred family. However, the visible slope of the clast is less steep, perhaps on account of space weathering. This precludes, for now, making a direct link. Hence, there is no direct evidence yet that the foreign clasts in Almahata Sitta are from the Mildred family.

Can the Original UPB Daughter Family Still Be Found?

Could there still be a recognizable family of daughter asteroids from the original catastrophic disruption of the UPB in the present-day asteroid belt? It seems unlikely, based on what is known about ureilite chronology. According to the model of Wilson et al. (2008), melting on the UPB started approximately 1 Myr after calcium-aluminum-rich inclusions (CAI), and ended 4.5–5.8 Myr after CAI. Isotopic closure of the ^{26}Al-^{26}Mg and ^{53}Mn-^{53}Cr systems occurred around this time, probably as a result of the catastrophic collision (Goodrich et al. 2010; Qin et al. 2010).

The formation time of Jupiter is estimated around 3.3 ± 2.6 Myr after the onset of fragmentation in the Main Belt (Bottke et al. 2005a; O'Brien et al. 2007). The growing Jupiter and Saturn subsequently dragged mean-motion and secular resonances through the belt, cleaning out 90–95% of the material (Raymond et al. 2006; Minton and Malhotra 2009), leaving a remnant of large >100 km asteroids from the primordial population (Bottke et al. 2005a, 2005b; Scott 2006; Morbidelli et al. 2009). With the loss of gas from the solar nebula 3–6 Myr after CAI, the remaining asteroids started a process of destruction in mutual collisions, and reaccumulation, creating the asteroid families. The survival of families from this early solar system epoch may be possible, but considerable work on this topic is needed before we can link a particular ancient family to the ureilites. Migration of Jupiter and the other gas giants continued to occur, long after destruction of the UPB, which finally is believed to have resulted in the time period of the lunar so-called "late heavy bombardment" approximately 3.9 Ga (Gomes et al. 2005; Tsiganis et al. 2005). Dynamical models show that tightly clustered orbits in the asteroid belt would have dispersed in eccentricity and inclination to an unknown degree as resonances swept across their orbits (Morbidelli et al. 2009).

Small (<100 km) asteroids with spectra similar to 2008 TC_3 are scattered throughout the inner and central belt (blue points in Fig. 8). Could these objects have originated from the UPB, whereas they are now dispersed throughout the Main Belt? Probably not. Notice how most are confined to low inclinations and positions just inside the 3:1 and 5:2 mean-motion resonances. They may, instead, signify debris from at least two progenitor bodies, one of which may be 335 Roberta. These dispersed families are presumably very old (>1 Gyr) and possibly lost many small fragments through the Yarkovsky effect. This would make this group a less efficient source of ureilites.

The Source Region of the UPB

It has been noticed before that among the asteroid families are surprisingly few shattered differentiated

asteroids, the Vesta family being the exception (Chapman 1986; Wetherhill and Chapman 1988; Gaffey 1993; Moskovitz et al. 2008). Because protoplanets can remain relatively long in a partially melted stage, partially melted parent bodies should have been a significant fraction of all protoplanetary bodies. Indeed, the diversity of iron meteorites suggests numerous shattered cores of differentiated parent bodies (e.g., Bottke et al. 2006). Although many $D > 100$ km planetesimals disrupted early in solar system history (Bottke et al. 2005a; Morbidelli et al. 2009), a representative sample of fragments is lacking. This lack has been explained by assuming that the many different iron meteorites originated instead from metallic cores of protoplanets formed very early during the formation of the solar system (< 1 Myr) and in regions closer to the Sun, where massive disruptions were common due to higher impact speeds (Bottke et al. 2006; Morbidelli et al. 2009; Raymond et al. 2009). Ureilites, too, were thought to have formed early in the solar system (< 1 Myr), but in the outer part of the asteroid belt (Scott 2006). The recrystallization into diamonds combined with rapid cooling rates (Herrin et al. 2010) suggests that the catastrophic disruption was particularly violent, involving either a relatively large impactor or relatively large impact speeds.

It is possible that the UPB originated in the terrestrial region of the solar system instead, around the time of embryo formation in this region, fragmented and reassembled there, and only later ended up in the asteroid belt as one of a number of large > 100 km F-class asteroids. The terrestrial planets accumulated and dispersed wandering protoplanets at least until the Moon-forming event at about 50 Myr. Where the UPB ended up remains unknown.

In that case, much of the UPB melting may be on account of impacts rather than radiogenic elements. Melting of the UPB may have occurred in a "hit and run" collision (Asphaug et al. 2006; Downes et al. 2008; Asphaug 2010). If barely grazing, the projectile would have been stripped of much of its crust, with the resultant composition of the surviving reaccreting debris potentially consistent with what we know of the UPB. If this event took place, it possibly occurred outside the asteroid belt, with protoplanets scattering some of the remnants of the UPB or the surviving UPB itself into the Main Belt zone (Bottke et al. 2006).

Evidence for an origin of the UPB in the terrestrial region may come, perhaps, from the numerous enstatite (and ordinary) chondrite clasts found in Almahata Sitta. These are thought to have formed from a much higher temperature region in the nebula than did the carbonaceous chondrites (e.g., Gaffey et al. 1993). These clasts may have mixed in with UPB fragments early in the evolution of the parent body, others only during subsequent collisions and reaccretions in the asteroid belt. The dominance of ordinary and enstatite chondrites being mixed in with the ureilites, as opposed to carbonaceous chondrites, puts this collisional history predominantly in the inner Main Belt or terrestrial region.

CONCLUSIONS

A population of low-inclination NEA has been identified with spectra similar to 2008 TC_3, within the uncertainties from composition variations recognized in Almahata Sitta alone. A second population of high-inclination objects was also found, with bluer spectra than asteroid 2008 TC_3, which probably derived from an unrelated source.

These populations originated most likely from one of the asteroid families in the Main Belt. Among the five-candidate F- and B-class asteroid families identified, the Theobalda family is a cratering family, too young to account for the CRE age of ureilites, and located in the outer Main Belt, resonances of which have a low probability of supplying asteroids to Earth. The Pallas and Themis families are discarded as a likely source region for 2008 TC_3 also, because of signs of hydration at the surface and distinctly different near-IR spectra. The Pallas family is identified as the likely source of the high-inclination F-class near-Earth object population instead.

The Hoffmeister family is dynamically young and was created in a supercatastrophic collision, creating many small fragments that now may be leaking into the J5:2 and J3:1 resonances. If the Gefion family is the source of L chondrites, then the Hoffmeister family could be the source of ureilites. The family is not a very efficient source for delivering meteorites in 2008 TC_3-like orbits, however, and the spectrum of 1726 Hoffmeister does not match that of Almahata Sitta.

Two potential source regions for the low-inclination population of NEA with 2008 TC_3-like spectra remain: the inner-belt population of dispersed asteroids and the Polana family. They are favored on dynamical grounds, because they have the potential to deliver asteroids efficiently on orbits like 2008 TC_3 through inner-belt resonances. Compared to 2008 TC_3, however, Polana family members have spectra with a more bluish slope, lower albedo, redder near-IR slope, and weak (or absent) pyroxene bands. Pending a better understanding of space weathering effects on ureilitic materials, these differences could point to compositional differences. Finally, a population of ungrouped asteroids scattered in the inner and central belt has optical spectra similar to 2008 TC_3, but generally lack near-IR spectra. The

one asteroid that does have a known near-IR spectrum, 335 Roberta, does not resemble 2008 TC_3 at near-IR wavelengths.

In future work, space weathering studies of ureilitic materials are needed to understand how the spectrum of the Main Belt progenitor may look different from the spectra of 2008 TC_3 and the Almahata Sitta meteorites. Observational studies should look for Main Belt asteroids that have a full 350–2500 nm spectra similar to 2008 TC_3. Small members of the Polana and Hoffmeister families may be good targets for this search. An alternative route to find the source region of the ureilites would be to search for asteroids with reflectance spectra similar to those of the foreign clasts in Almahata Sitta, which must have sampled the local collisional environment. Note, however, that the clasts do not sample the present-day population of small chondrites, because they were accreted long ago. Finally, spectroscopy of the large isolated F-class asteroids in Table 2 may identify other formerly partially molten protoplanets that now have lost their mantle from collisions with smaller asteroids.

Acknowledgments—This article was improved greatly from comments by referees Alberto Cellino, Edward Scott, David W. Mittlefehldt, and associate editor Cyrena Goodrich. We also thank Lucy McFadden for helpful discussions, and Beth E. Clark and Schelte J. Bus for sharing published data. We thank the many students and staff of the University of Khartoum for their support in recovering the meteorites. The near-IR spectra discussed in this article were measured at the IRTF telescope at Manua Kea, Hawaii in October and November of 2009, as part of the MIT-UH-IRTF Joint Campaign for NEO Spectral Reconnaissance. All of the data utilized in this publication (unless so specified) were obtained and made available by the MIT-UH-IRTF Joint Campaign for NEO Reconnaissance. The IRTF is operated by the University of Hawaii under Cooperative Agreement no. NCC 5-538 with the National Aeronautics and Space Administration, Office of Space Science, Planetary Astronomy Program. The MIT component of this work is supported by the National Science Foundation under Grant No. 0506716. M. E. Z. acknowledges support from the Hayabusa program. P. J. is supported by a grant from the NASA Planetary Astronomy Program.

Editorial Handling Dr. Cyrena Goodrich

REFERENCES

Asphaug E. 2010. Similar-sized collisions and the diversity of planets. *Chemie der Erde—Geochemistry* 70:199–219.

Asphaug E., Agnor C. B., and Williams Q. 2006. Hit-and-run planetary collisions. *Nature* 439:155–160.

Aylmer D., Vogt S., Herzog G. F., Klein J., Fink D., and Middleton R. 1990. Low ^{10}Be and ^{26}Al contents of ureilites: Production at meteoroid surfaces. *Geochimica et Cosmochimica Acta* 54:1775–1784.

Belskaya I. N., Shkuratov Yu G., Efimov Yu S., Shakhovskoy N. M., Gil-Hutton R., Cellino A., Zubko E. S., Ovcharenko A. A., Bondarenko S. Yu., Shevchenko V. G., Fornasier S., and Barbieri C. 2005. The F-type asteroids with small inversion angles of polarization. *Icarus* 178:213–221.

Berkley J. L., Taylor G. J., Keil K., Harlow G. E., and Prinz M. 1980. The nature and origin of ureilites. *Geochimica et Cosmochimica Acta* 44:1579–1597.

Binzel R. P., Morbidelli A., Merouane S., DeMeo F. E., Brilan M., Vernazza P., Thomas C. A., Rivkin A. S., Bus S. J., and Tokunaga A. T. 2010a. Earth encounters as the origin of fresh surfaces on near-Earth asteroids. *Nature* 463:331–334.

Binzel R. P., Thomas C. A., Rivkin A. S., Burbine T. H., and Bus S. J. 2010b. SMAS: Small Main-Belt Asteroid Spectroscopic Survey. MIT website: http://smass.mit.edu/smass.html. Accessed August 2010.

Bottke W. F., Vokrouhlicky D., Rubincam D. P., and Broz M. 2002a. The effect of Yarkovsky thermal forces on the evolution of asteroids and meteoroids. In *Asteroids III*, edited by Bottke W. F., Cellino A., Paolicchi P., and Binzel R. P. Tucson, AZ: The University of Arizona Press. pp. 395–407.

Bottke W. F., Morbidelli A., Jedicke R., Petit J.-M., Levison H. F., Michel P., and Metcalfe T. S. 2002b. Debiased orbital and absolute magnitude distribution of the near-Earth objects. *Icarus* 156:399–433.

Bottke W. F., Durda D. D., Nesvorný D., Jedicke R., Morbidelli A., Vokrouhlicky D., and Levison H. 2005a. Linking the collisional history of the main asteroid belt to its dynamical excitation and depletion. *Icarus* 179:63–94.

Bottke W. F., Durda D. D., Nesvorný D., Jedicke R., Morbidelli A., Vokrouhlicky D., and Levison H. 2005b. The fossilized size distribution of the main asteroid belt. *Icarus* 175:111–140.

Bottke W. F., Nesvorný D., Grimm R. E., Morbidelli A., and O'Brien D. P. 2006. Iron meteorites as remnants of planetesimals formed in the terrestrial planet region. *Nature* 439:821–824.

Britt D. T., Tholen D. J., Bell J. F., and Pieters C. M. 1992. Comparison of asteroid and meteorite spectra: Classification by principal component analysis. *Icarus* 99:153–166.

Britt D. T., Rivkin A. S., Howell E. S., and Lebofsky L. A. 1994. 'Wet' E and M class asteroids (abstract). *Meteoritics* 29:A450.

Brunetto R., Vernazza P., Marchi S., Birlan M., Fulchignoni M., Orofino V., and Strazzulla G. 2006. Modeling asteroid surfaces from observations and irradiation experiments: The case of 832 Karin. *Icarus* 184:327–337.

Burbine T. H., Buchanan P. C., Binzel R. P., Bus S. J., Hiroi T., Hinrichs J. L., Meibom A., and McCoy T. J. 2001. Vesta, Vestoids, and the howardite, eucrite, diogenite group: Relationships and the origin of spectral differences. *Meteoritics & Planetary Science* 36:761–781.

Burbine T. H., McCoy T. J., Meibom A., Gladman B., and Keil K. 2002. Meteoritic parent bodies: Their number and identification. In *Asteroids III*, edited by Bottke W. F., Cellino A., Paolicchi P., and Binzel R. P. Tucson, AZ: The University of Arizona Press. pp. 653–667.

Bus S. J. 1999. Compositional structure in the asteroid belt: Results of a spectroscopic survey. Ph.D. thesis, Massachusetts Institute of Technology, Cambridge, Massachusetts.

Bus S. J. and Binzel R. P. 2002. Phase II of the Small Main-Belt Asteroid Spectroscopic Survey: A feature-based taxonomy. *Icarus* 158:146–177.

Campins H., Hargrove K., Pinilla-Alonso N., Howell E. S., Kelley M. S., Licandro J., Mothé-Diniz T., Fernández Y., and Ziffer J. 2010. Water ice and organics on the surface of the asteroid 24 Themis. *Nature* 464:1320–1321.

Cellino A. 2004. Minor bodies: Spectral gradients and relationships with meteorites. *Space Science Reviews* 92:397–412.

Cellino A., Zappalà V., Doressoundiram A., Di Martino M., Bendjoya Ph., Dotto E., and Migliorini F. 2001. The puzzling case of the Nysa-Polana Family. *Icarus* 152:225–237.

Cellino A., Bus S. J., Doressoundiram A., and Lazzaro D. 2002. Spectroscopic properties of asteroid families. In *Asteroids III*, edited by Bottke W. F., Cellino A., Paolicchi P., and Binzel R. P. Tucson, AZ: The University of Arizona Press. pp. 633–643.

Chapman C. R. 1986. Implications of the inferred compositions of asteroids for their collisional evolution. *Memorie Società Astronomica Italiana* 57:103–114.

Clark B. E., Fanale F. P., and Salisbury J. W. 1992. Meteorite-asteroid spectral comparison: The effects of comminution, melting, and recrystallization. *Icarus* 97:288–297.

Clark B. E., Helfenstein P., Bell J. F., Peterson C., Ververka J., Izenberg N. I., Domingue D., Wellnitz D., and McFadden L. 2002. NEAR infrared spectrometer photometry of asteroid 433 Eros. *Icarus* 155:189–204.

Clark B. E., Bus S. J., Rivkin A. S., McConnochie T., Sanders J., Shah S., Hiroi T., and Shepard M. 2004. E-type asteroid spectroscopy and compositional modeling. *Journal of Geophysical Research* 109:CiteID E02001.

Clark B. E., Ockert-Bell M. E., Clautis E. A., Nesvorný D., Mothé-Diniz T., and Shelte B. J. 2009. Spectroscopy of K-complex asteroids: Parent bodies of carbonaceous meteorites? *Icarus* 202:119–133.

Clark B. E., Ziffer J., Nesvorný D., Campins H., Rivkin A. S., Hiroi T., Barucci M. A., Fulchignoni M., Binzel R. P., Fornasier S., DeMeo F., Ockert-Bell M. E., Licandro J., and Mothé-Diniz T. 2010. Spectroscopy of B-type asteroids: Subgroups and meteorite analogs. *Journal of Geophysical Research* 115:CiteID E06005.

Cloutis E. A., Hudon P., Romanek C. S., Gaffey M. J., and Hardersen P. S. 2010. Spectral reflectance properties of ureilites. *Meteoritics & Planetary Science* 45. This issue.

Croft S. K., McNamara D. H., and Feltz K. A. 1972. The (B-V) and (U-B) color indices of the Sun. *Publications of the Astronomical Society of the Pacific* 84:515–518.

DeLeón J., Campins H., Tsiganis K., Morbidelli A., and Licandro J. 2010. Origin of the near-Earth asteroid Phaethon and the Geminids meteor shower. *Astronomy & Astrophysics* 513:A26.

DeMeo F. E., Binzel R. P., Slivan S. M., and Bus S. J. 2009. An extension of the Bus asteroid taxonomy into the near-infrared. *Icarus* 202:160–180.

Dodd R. T. 1981. *Meteorites: A petrologic-chemical synthesis*. Cambridge, UK: Cambridge University Press. pp. 293–304.

Downes H., Mittlefehldt D. W., Herrin J. S., and Hudon P. 2007. Accretion, differentiation and impact processes on the ureilite parent body (abstract #1620). 38th Lunar and Planetary Science Conference. CD-ROM.

Downes H., Mittlefehldt D. W., Kita N. T., and Valley J. W. 2008. Evidence from polymict ureilite meteorites for a disrupted and re-accreted single ureilite parent asteroid gardened by several distinct impactors. *Geochimica et Cosmochimica Acta* 72:4825–4844.

Duffard R., Lazzaro D., Licandro J., De Sanctis M. C., Capria M. T., and Carvano J. M. 2004. Mineralogical characterization of some basaltic asteroids in the neighborhood of (4) Vesta: First results. *Icarus* 171:120–132.

Dumas C., Owen T., and Barucci M. A. 1998. Near-infrared spectroscopy of low-albedo surfaces of the solar system: Search for the spectral signature of dark material. *Icarus* 133:221–232.

Durda D. D., Bottke W. F., Nesvorný D., Enke B. L., Merline W. J., Aspaug E., and Richardson D. C. 2007. Size frequency distibution of fragments from SPH/N-body simulations of asteroid impacts: Comparison with observed asteroid families. *Icarus* 186:498–516.

Fevig R. A. and Fink U. 2007. Spectral observations of 19 weathered and 23 fresh NEA and their correlation with orbital parameters. *Icarus* 188:175–188.

Fornasier S., Clark B. E., Dotto E., Migliorini A., Ockert-Bell M., and Barucci M. A. 2010. Spectroscopic survey of M-type asteroids. *Icarus* 210:655–673.

Friedrich J. M., Wolf S. F., Rumble D., Troiano J., Gagnon C. J. L., Jenniskens P., and Shaddad M. H. 2010. The elemental composition of Almahata Sitta. *Meteoritics & Planetary Science* 45. This issue.

Gaffey M. J. 1993. Forging an asteroid-meteorite link. *Science* 260:167–168.

Gaffey M. J., Bell J., and Cruikshank D. P. 1990. Reflectance spectroscopy and asteroid surface mineralogy. In *Asteroids II*, edited by Binzel R. P., Gehrels T., and Matthews M. S. Tucson, AZ: The University of Arizona Press. pp. 98–127.

Gaffey M. J., Burbine T. H., and Binzel R. P. 1993. Asteroid spectroscopy: Progress and perspectives. *Meteoritics & Planetary Science* 28:161–187.

Gallardo T. 2007. The Mars 1:2 resonant population. *Icarus* 190:280–282.

Gladman B. J., Burns J. A., Duncan M., Lee P., and Levison H. F. 1996. The exchange of impact ejecta between terrestrial planets. *Science* 271:1387–1392.

Gladman B. J., Migliorini F., Morbidelli A., Zappala V., Michel P., Cellino A., Froeschle C., Levison H. F., Bailey M., and Duncan M. 1997. Dynamical lifetimes of objects injected into asteroid belt resonances. *Science* 277:197–201.

Gomes R., Levison H. F., Tsiganis K., and Morbidelli A. 2005. Origin of the cataclysmic Late Heavy Bombardment period of the terrestrial planets. *Nature* 435:466–469.

Goodrich C. A. 1992. Ureilites: A critical review. *Meteoritics* 27:327–352.

Goodrich C. A. 2004. Ureilitic breccias: Clues to the petrologic structure and impact disruption of the ureilite parent asteroid. *Chemie der Erde* 64:283–327.

Goodrich C. A., Van Orman J. A., and Wilson L. 2007. Fractional melting and smelting on the ureilite parent body. *Geochimica et Cosmochimica Acta* 71:2876–2895.

Goodrich C. A., Hutcheon I. D., Kita N. T., Huss G. R., Cohen B. A., and Keil K. 2010. ^{53}Mn-^{53}Cr and ^{26}Al-^{26}Mg ages of a feldspathic lithology in polymict ureilites. *Earth and Planetary Science Letters* 295:531–540.

Gray D. F. 1992. The inferred color index of the Sun. *Publications of the Astronomical Society of the Pacific* 104:1035–1038.

Hapke B. 2001. Space weathering from Mercury to the asteroid belt. *Journal of Geophysical Research* 106:10,039–10,074.

Herrin J. S., Zolensky M. E., Ito M., Le L., Mittlefehldt D. W., Jenniskens P., and Shaddad M. H. 2010. Thermal and fragmentation history of ureilitic asteroids; Insights from the Almahata Sitta fall. *Meteoritics & Planetary Science* 45. This issue.

Hiroi T., Pieters C. M., Zolensky M. E., and Lipschutz M. E. 1993. Evidence of thermal metamorphism on the C, G, B, and F asteroids. *Science* 261:1016–1018.

Hiroi T., Ohashi H., and Otake H. 1999. Simulation of space weathering of planet-forming materials: Nanosecond pulse laser irradiation and proton implantation on olivine and pyroxene samples. *Earth, Planets and Space* 51:1255–1265.

Hiroi T., Zolensky M. E., and Pieters C. M. 2001. Discovery of the first D-asteroid spectral counterpart: Tagish Lake meteorite (abstract #1776). 32nd Lunar and Planetary Science Conference. CD-ROM.

Hiroi T., Jenniskens P., Bishop J. L., Shatir T. S. M., and Kudoda A. M. 2010. Bidirectional visible-NIR and biconical FT-IR reflectance spectra of Almahata Sitta meteorite samples. *Meteoritics & Planetary Science* 45. This isuse.

Jenniskens P. 2006. *Meteor showers and their parent comets*. Cambridge, UK: Cambridge University Press. 790 p.

Jenniskens P., Borovička J., Betlem H., Ter Kuile C., Bettonvil F., and Heinlein D. 1992. Orbits of meteorite producing fireballs: The Glanerbrug—A case study. *Astronomy & Astrophysics* 255:373–376.

Jenniskens P., Shaddad M. H., Numan D., Elsir S., Kudoda A. M., Zolensky M. E., Le L., Robinson G. A., Friedrich J. M., Rumble D., Steele A., Chesley S. R., Fitzsimmons A., Duddy S., Hsieh H. H., Ramsay G., Brown P. G., Edwards W. N., Tagliaferri E., Boslough M. B., Spalding R. E., Dantowitz R., Kozubal M., Pravec P., Borovička J., Charvat Z., Vaubaillon J., Kuiper J., Albers J., Bishop J. L., Mancinelli R. L., Sandford S. A., Milam S. N., Nuevo M., and Worden S. P. 2009. The impact and recovery of asteroid 2008 TC_3. *Nature* 458:485–488.

Jewitt D. and Hsieh H. 2006. Physical observations of 2005 UD: A mini-Phaethon. *The Astronomical Journal* 132:1624–1629.

Johnson H. L. and Morgan W. W. 1953. Fundamental stellar photometry for standards of spectral type on the revised system of the Yerkes spectral atlas. *The Astrophysical Journal* 117:313–352.

Jones T. D., Lebofsky L. A., Lewis J. S., and Marley M. S. 1990. The composition and origin of the C, P, and D asteroids: Water as a tracer of thermal evolution in the outer belt. *Icarus* 88:172–192.

Juric M., Ivezic Z., Lupton H. R., Quinn T., Tabachnik S., Fan X., Gunn J. E., Hennessy G. S., Knapp G. R., Munn J. A., Pier J. R., Rockosi C. M., Schneider D. P., Brinkmann J., Csabai I., and Fukugita M. 2002. Comparison of asteroids observed in the SDSS with a catalog of known asteroids. *The Astronomical Journal* 124:1776–1787.

Kelley M. S., Gaffey M. J., and Williams J. G. 1994. Compositional evidence in favor of a genetic link between the Nysa and Herta asteroid families (abstract). 25th Lunar and Planetary Science Conference. p. 689.

Kinoshita D., Ohtsuka K., Sekiguchi T., Watanabe J., Ito T., Arakida H., Kasuga T., Miyasaka S., Nakamura R., and Lin H.-C. 2007. Surface heterogeneity of 2005 UD from photometric observations. *Astronomy & Astrophysics* 466:1153–1158.

Knezevic Z. and Milani A. 2003. Proper element catalogs and asteroid families. *Astronomy & Astrophysics* 403:1165–1173.

Knezevic Z., Milani A., Farinella P., Froeschle Ch., and Froeschle Cl. 1991. Secular resonances from 2 to 50 AU. *Icarus* 93:316–330.

Kowalski R. A. 2008. 2008 TC_3. In *MPEC 2008–T50*, edited by Williams G. V. Cambridge, MA: Minor Planet Center, Smithsonian Astrophysical Observatory. p. 1.

Lebofsky L. A. 1980. Infrared reflectance spectra of asteroids—A search for water of hydration. *The Astronomical Journal* 85:573–585.

Lebofsky L. A., Jones T. D., Owensby P. D., Feierberg M. A., and Consolmagno G. J. 1990. The nature of low-albedo asteroids from 3-micron multi-color photometry. *Icarus* 83:16–26.

Licandro J., Campins H., Mothé-Dinaz T., Pinilla-Alonso N., and de León J. 2007. The nature of comet-asteroid transition object (3200) Phaethon. *Astronomy & Astrophysics* 461:751–757.

Manara A., Covino S., and Di Martino M. 2001. Visual spectroscopy of asteroids at San Pedro Martir. *Revista Mexicana de Astronomía y Astroísica* 37:35–38.

Marchi S., Paolicchi P., Lazzarin M., and Magrin S. 2006. A general spectral slope—Exposure relation for S-type Main Belt and near-Earth asteroids. *The Astronomical Journal* 131:1138–1141.

McFadden L. A., Gaffey M. J., and McCord T. B. 1984. Mineralogical-petrological characterization of near-Earth asteroids. *Icarus* 59:25–40.

Migliorini F., Manara A., di Martino M., and Farinella P. 1996. The Hoffmeister asteroid family: Inferences from physical data. *Astronomy & Astrophysics* 310:681–685.

Migliorini F., Morbidelli A., Zappala V., Gladman B. J., Bailey M. E., and Cellino A. 1997. Vesta fragments from ν6 and 3:1 resonances: Implications for V-type near-Earth asteroids and howardite, eucrite and diogenite meteorites. *Meteoritics & Planetary Science* 32: 903–916.

Minton D. A. and Malhotra R. 2009. A record of planet migration in the main asteroid belt. *Nature* 457:1109–1111.

Mittlefehldt D. W. 2005. Achondrites. In *Meteorites, comets and planets*, edited by Davis A. M. Treatise on

geochemistry, vol. 1, Amsterdam: Elsevier B. V. pp. 291–324.

Mittlefehldt D. W., McCoy T. J., Goodrich C. A., and Kracher A. 1998. Non-chondritic meteorites from asteroidal bodies. In *Planetary materials*, edited by Papike J. J. Washington, D.C.: Mineralogical Society of America pp. 1–195.

Morbidelli A., Bottke W. F., Nesvorný D., and Levison H. F. 2009. Asteroids were born big. *Icarus* 204:558–573.

Moskovitz N. A., Jedicke R., Gaidos E., Willman M., Nesvorný D., Fevig R., and Ivezic Z. 2008. The distribution of basaltic asteroids in the main belt. *Icarus* 198:77–90.

Moskovitz N., Willman M., Burbine T., Binzel R., and Bus S. 2010. A spectroscopic comparison of HED meteorites and V-type asteroids in the inner main belt. *Icarus* 208:773–788.

Mothé-Diniz T. and Nesvorný D. 2008. Visible spectroscopy of extremely young asteroid families. *Astronomy & Astrophysics* 486:L9–L12.

Mothé-Diniz T., Roig F., and Carvano J. M. 2005. Reanalysis of asteroid families structure through visible spectroscopy. *Icarus* 174:54–80.

Nesvorný D., Jedicke R., Whiteley R. J., and Zeljko I. 2005. Evidence for asteroid space weathering from the Sloan Digital Sky Survey. *Icarus* 173:132–152.

Nesvorný D., Bottke W. F., Vokroughlicky D., Morbidelli A., and Jedicke R. 2006a. Asteroid families. In *Proceedings of IAU Symposium, No. 229*, edited by Lazzaro D., Ferraz-Mello S., and Fernandez J. A. Cambridge, UK: Cambridge University Press. pp. 289–299.

Nesvorný D., Enke B. L., Bottke W. F., Durda D. D., Aspaug E., and Richardson D. C. 2006b. Karin cluster formation by asteroid impact. *Icarus* 183:296–311.

Nesvorný D., Vokrouhlicky D., Morbidelli A., and Bottke W. F. 2009. Asteroidal source of L chondrite meteorites. *Icarus* 200:698–701.

Noble S. K. and Pieters C. M. 2003. Preservation of space weathering products in regolith breccias (abstract). *Meteoritics & Planetary Science* 38:A5098.

Novakovic B. 2010. Portrait of Theobalda as a young asteroid family. *Monthly Notices of the Royal Astronomical Society* 407:1477–1486.

O'Brien D. P., Morbidelli A., and Bottke W. F. 2007. The primordial excitation and clearing of the asteroid belt revisited. *Icarus* 191:343–452.

Ohtsuka K. 2005. *2005 UD and the daytime Sextantids*. CBET 283. Cambridge, MA: Minor Planet Center. p. 1.

Ohtsuka K., Nakato A., Nakamura T., Kinoshita D., Ito T., Yoshikawa M., and Hasegawa S. 2009. Solar-radiation heating effects on 3200 Phaethon. *Publications of the Astronomical Society of Japan* 61:1375–1387.

Pieters C. M., Fischer E. M., Rode O., and Basu A. 1993. Optical effects of space weathering: The role of the finest fraction. *Journal of Geophysical Research* 98:20817–20824.

Pieters C. M., Taylor L. A., Noble S. K., Keller L. P., Hapke B., Morris R. V., Allen C. C., McKay D. S., and Wentworth S. 2000. Space weathering on airless bodies: Resolving a mystery with lunar samples. *Meteoritics & Planetary Science* 35:1101–1107.

Qin L., Rumble D., Alexander C. M. O'D., Carlson R. W., Jenniskens P., and Shaddad M. H. 2010. The chromium isotopic composition of Almahata Sitta. *Meteoritics & Planetary Science* 45. This issue.

Rankenburg K., Humayun M., Brandon A. D., and Herrin J. S. 2008. High siderophile elements in ureilites. *Geochimica et Cosmochimica Acta* 72:4642–4659.

Raymond S. N., Quinn T., and Lunine J. I. 2006. High-resolution simulations of the final assembly of Earth-like planets I. Terrestrial accretion and dynamics. *Icarus* 183:265–282.

Raymond S. N., O'Brien D. P., Morbidelli A., and Kaib N. A. 2009. Building the terrestrial planets: Constrained accretion in the inner solar system. *Icarus* 203:644–662.

Rayner J. T., Toomey D. W., Onaka P. M., Denault A. J., Stahlberger W. E., Vacca W. D., Cushing M. C., and Wang S. 2003. SpeX: A medium-resolution 0.8-5.5 micron spectrograph and imager for the NASA infrared telescope facility. *Publications of the Astronomical Society of the Pacific* 115:362–382.

Rivkin A. S., Howell E. S., Britt D. T., Lebosfsky L. A., Nolan M. C., and Branston D. D. 1995. Three-micron spectrometric survey of M- and E-class asteroids. *Icarus* 117:90–100.

Rivkin A. S., Davies J. K., Johnson J. R., and Lebofsky L. A. 1996. High resolution spectra of hydrated asteroids in the three-micron region (abstract). *Meteoritics & Planetary Science* 31:A116.

Rivkin A. S., Howell E. S., Lebofsky L. A., Clark B. E., and Britt D. T. 2000. The nature of M-class asteroids from 3-micron observations. *Icarus* 145:351–368.

Rivkin A. S., Howell E. S., Vilas F., and Lebofsky L. A. 2002. Hydrated minerals on asteroids: The astronomical record. In *Asteroids III*, edited by Bottke W. F. Jr., Cellino A., Paolicchi P., and Binzel R. P. Tucson, AZ: The University of Arizona Press. pp. 235–253.

Rosenbush V. K., Sherchenko V. G., Kiselev M. N., Sergeev A. V., Shakhovskoy N. M., Velichko F. P., Kolesnikov S. V., and Karpov N. V. 2009. Polarization and brightness opposition effects for the E-type asteroid 44 Nysa. *Icarus* 201:655–665.

Rumble D., Zolensky M. E., Friedrich J. M., Jenniskens P., and Shaddad M. H. 2010. The oxygen isotope composition of Almahata Sitta. *Meteoritics & Planetary Science* 45. This issue.

Sabbah H., Morrow A. L., Jenniskens P., Shaddad M. H., and Zare R. N. 2010. Polycyclic aromatic hydrocarbons in asteroid 2008 TC_3: Dispersion of organic compounds inside asteroids. *Meteoritics & Planetary Science* 45. This issue.

Sandford S. A. 1993. The mid-infrared transmission spectra of Antarctic ureilites. *Meteoritics* 28:579–585.

Sandford S. A., Milam S. N., Nuevo M., Jenniskens P., and Shaddad M. H. 2010. The mid-infrared transmission spectra of multiple stones from the Almahata Sitta meteorite. *Meteoritics & Planetary Science* 45. This issue.

Sasaki S., Kurahashi E., Nakamura K., Hiroi T., and Yamanaka C. 2002. Laboratory simulation of space weathering: TEM and ESR confirmation of nanophase iron particles and change of optical properties of regolith. *European Space Agency Special Publication* 92:929–931.

Sawyer S. 1998. *Sawyer asteroid spectra*. EAR-A-3-RDR-SAWYER-ASTEROID-SPECTRA-V1.2. NASA Planetary Data System College Park, MD: University of Maryland.

Scheirich P., Durech J., Pravec P., Kozubal M., Dantowitz R., Kaasalainen M., Betzler A. S., Beltrame P., Muler G., Birtwhistle P., and Kugel F. 2010. The shape and rotation of asteroid 2008 TC_3. *Meteoritics & Planetary Science*. 45 This issue.

Schmidt B. E., Thomas P. C., Bauer J. M., Li Y.-Y., McFadden L. A., Mutchler M. J., Radcliffe S. C., Rivkin A. S., Russell C. T., Parker J. Wm., and Stern S. A. 2009. The shape and surface variation of 2 Pallas from the Hubble Space Telescope. *Science* 326:275–278.

Scott E. R. D. 2006. Meteoritical and dynamical constraints on the growth mechanisms and formation times of asteroids and Jupiter. *Icarus* 185:72–82.

Shaddad M. H., Jenniskens P., Numan D., Kudoda A. M., Elsir S., Riyad I. F., Elkareem A., Alameen M., Alameen N. M., Eid O., Osman A. T., AbuBaker M. I., Chesley S. R., Chodas P. W., Albers J., Edwars W. N., Brown P. G., Kuiper J., and Friedrich J. M. 2010. The recovery of asteroid 2008 TC_3. *Meteoritics & Planetary Science* 45. This issue.

Shepard M. K., Clark B. E., Nolan M. C., Howell E. S., Magri C., Giorgini J. D., Benner L. A. M., Ostro S. J., Harris A. W., Warner B., Pray D., Pravec P., Fauerbach M., Bennett T., Klotz A., Behrend R., Correia H., Coloma J., Casulli S., and Rivkin A. 2008. A radar survey of M- and X-class asteroids. *Icarus* 195:184–205.

Shepard M. K., Clark B. E., Ockert-Bell M., Nolan M. C., Howell E. S., Magri C., Giorgini J. D., Benner L. A. M., Ostro S. J., Harris A. W., Warner B. D., Stephens R. D., and Mueller M. 2009. AAS DPS meeting #41, Fajardo, Puerto Rico, October 4–9. 43.12 (abstract).

Singletary S. J. and Grove T. L. 2003. Early petrologic processes on the ureilite parent body. *Meteoritics & Planetary Science* 38:95–108.

Straizys V. and Valiauga G. 1994. Color indices of the Sun in the Vilnius and the UBV system. *Baltic Astronomy* 3:282–291.

Strazzulla G., Dotto E., Binzel R., Brunetto R., Barucci M. A., Bianco A., and Orofino V. 2004. Spectral alteration of the meteorite Epinal (H5) induced by heavy ion irradiation: A simulation of space weathering effect on near-Earth asteroids. *Icarus* 174:31–35.

Takeda H. 1987. Mineralogy of Antarctic ureilites and a working hypothesis for their origin and evolution. *Earth and Planetary Science Letters* 81:358–370.

Takeda H., Mori H., and Ogata H. 1989. Mineralogy of augite-bearing ureilites and the origin of their chemical trends. *Meteoritics* 24:73–81.

Tedesco E. F. 1994. IRAS minor planet survey. In *Asteroids, comets, meteors 1993*, edited by Milani A., Di Martino M., and Cellino A. Dordrecht: Kluwer. pp. 463–466.

Tedesco E. F., Gradie J., Tholen D. J., and Zellner B. 1982a. The Nysa family: Remnants of a strongly differentiated asteroid? *Bulletin of the American Astronomical Society* 14:720.

Tedesco E. F., Tholen D. J., and Zellner B. 1982b. The eight-color asteroid survey: Standard stars. *The Astronomical Journal* 87:1585–1592.

Tholen D. J. 1984. Asteroid taxonomy from cluster analysis of photometry. Ph.D. thesis, The University of Arizona, Tucson, Arizona.

Tholen D. J. and Barucci M. A. 1989. Asteroid taxonomy. In *Asteroids II*, edited by Binzel R., Gehrels T., and Matthews M. Tucson, AZ: The University of Arizona Press. pp. 298–315.

Tsiganis K., Gomes R., Morbidelli A., and Levison H. F. 2005. Origin of the orbital architecture of the giant planets of the solar system. *Nature* 435:459–461.

Tupieva F. A. 2003. UBV photometry of asteroid 44 Nysa. *Astronomy & Astrophysics* 408:379–385.

Vdovykin G. P. 1970. Ureilites. *Space Science Reviews* 10:483–510.

Vernazza P., Brunetto R., Binzel R. P., Perron C., Fulvio D., Strazzulla G., and Fulchignoni M. 2009. Plausible parent bodies for enstatite chondrites and mesosiderites: Implications for Lutetia's flyby. *Icarus* 202:477–486.

Vokrouhlicky D., Broz M., Bottke W. F., Nesvorný D., and Morbidelli A. 2006. Yarkovsky/YORP chronology of asteroid families. *Icarus* 182:118–142.

Warren P. H. 2010. Asteroidal depth-pressure relationships and the style of ureilite anatexis (abstract). *Meteoritics & Planetary Science* 42:A5320.

Warren P. H. and Huber H. 2006. Ureilite petrogenesis: A limited role for smelting during anatexis and catastrophic disruption. *Meteoritics* 41:835–849.

Warren P. H. and Kallemeyn G. W. 1992. Explosive volcanism and the graphite-oxygen fugacity buffer on the parent asteroid(s) of the ureilite meteorites. *Icarus* 100:110–126.

Welten K., Meier M. M. M., Caffee M. W., Nishizumi K., Wieler R., Jenniskens P., and Shaddad M. H. 2010. Cosmic nuclides in Almahata Sitta ureilite: Cosmic-ray exposure age, pre-atmospheric mass and bulk density of asteroid 2008 TC_3. *Meteoritics & Planetary Science* 45. This issue.

Wetherhill G. W. and Chapman C. R. 1988. Asteroids and meteorites. In *Meteorites and the early solar system*, edited by Kerridge J. F. and Matthews M. S. Tucson, AZ: The University of Arizona Press. pp. 35–67.

Willman M., Jedicke R., Moskovitz N., Nesvorný D., Vokrouhlicky D., and Mothé-Diniz T. 2010. Using the youngest asteroid clusters to constrain the space weathering and gardening rate on S-complex asteroids. *Icarus* 208:758–772.

Wilson L., Goodrich C. A., and van Orman J. A. 2008. Thermal evolution and physics of melt extraction on the ureilite parent body. *Geochimica et Cosmochimica Acta* 72:6154–6176.

Wisdom J. 1987. Chaotic behaviour in the solar system. *Proceedings of the Royal Society of London, A* 413:109–129.

Yang B. and Jewitt D. 2010. Identification of magnetite in B-type asteroids. *The Astronomical Journal* 140:692–698.

Zappalà V., Cellino A., Farinella P., and Milani A. 1994. Asteroid families. II. Extension to unnumbered multiopposition asteroids. *The Astronomical Journal* 107: 772–801.

Zappalà V., Bendjoya Ph., Cellino A., Farinella P., and Froeschle C. 1995. Asteroid families: Search of a 12,487-asteroid sample using two different clustering techniques. *Icarus* 116:291–314.

Zappalà V., Bendjoya Ph., Cellino A., Farinella P., and Froschle C. 1997. *Asteroid dynamical families*. EAR-A-5-DDR-FAMILY-V4.1. NASA Planetary Data System. College Park, MD: University of Maryland.

Zellner B., Tholen D. J., and Tedesco E. F. 1985. The eight-color asteroid survey: Results for 589 minor planets. *Icarus* 61:355–416.

Zolensky M., Herrin J., Mikouchi T., Ohsumi K., Friedrich J., Steele A., Rumble D., Fries M., Sandford S., Milam S., Hagiya K., Takeda H., Satake W., Kurihara T., Colbert M., Hanna R., Maisano J., Ketcham R., Goodrich C., Le L., Robinson G.-A., Martinez J., Ross K., Jenniskens P., and Shaddad M. 2010. Mineralogy and petrography of the Almahata Sitta ureilite. *Meteoritics & Planetary Science* 45. This issue.